Cell. Mol. Life Sci. (2014) 71:517–538
DOI 10.1007/s00018-013-1401-6

Cellular and Molecular Life Sciences

RESEARCH ARTICLE

The nucleotide-binding proteins Nubp1 and Nubp2 are negative regulators of ciliogenesis

Elena Kypri · Andri Christodoulou · Giannis Maimaris · Mette Lethan · Maria Markaki · Costas Lysandrou · Carsten W. Lederer · Nektarios Tavernarakis · Stefan Geimer · Lotte B. Pedersen · Niovi Santama

Received: 4 January 2013 / Revised: 3 June 2013 / Accepted: 6 June 2013 / Published online: 27 June 2013

Abstract Nucleotide-binding proteins Nubp1 and Nubp2 are MRP/MinD-type P-loop NTPases with sequence similarity to bacterial division site-determining proteins and are conserved, essential proteins throughout the Eukaryotes. They have been implicated, together with their interacting minus-end directed motor protein KIFC5A, in the regulation of centriole duplication in mammalian cells. Here we show that Nubp1 and Nubp2 are integral components of centrioles throughout the cell cycle, recruited independently of KIFC5A. We further demonstrate their localization at the basal body of the primary cilium in quiescent vertebrate cells or invertebrate sensory cilia, as well as in the motile cilia of mouse cells and in the flagella of *Chlamydomonas*. RNAi-mediated silencing of *nubp-1* in *C. elegans* causes the formation of morphologically aberrant and additional cilia in sensory neurons. Correspondingly, downregulation of Nubp1 or Nubp2 in mouse quiescent NIH 3T3 cells markedly increases the number of ciliated cells, while knockdown of KIFC5A dramatically reduces ciliogenesis. Simultaneous double silencing of Nubp1 + KIFC5A restores the percentage of ciliated cells to control levels. We document the normal ciliary recruitment, during these silencing regimes, of basal body proteins critical for ciliogenesis, namely CP110, CEP290, cenexin, Chibby, AurA, Rab8, and BBS7. Interestingly, we uncover novel interactions of Nubp1 with several members of the CCT/TRiC molecular chaperone complex, which we find enriched at the basal body and recruited independently of the Nubps or KIFC5A. Our combined results for Nubp1, Nubp2, and KIFC5A and their striking effects on cilium formation suggest a central regulatory role for these proteins, likely involving CCT/TRiC chaperone activity, in ciliogenesis.

Keywords Ciliogenesis · Molecular chaperones · Motor proteins · CCT/TRiC complex · Primary cilium

E. Kypri, A. Christodoulou, and G. Maimaris contributed equally to the experimental work.

Electronic supplementary material The online version of this article (doi:10.1007/s00018-013-1401-6) contains supplementary material, which is available to authorized users.

E. Kypri · A. Christodoulou · G. Maimaris · C. Lysandrou · N. Santama (✉)
Department of Biological Sciences, University of Cyprus, University Avenue 1, 1678 Nicosia, Cyprus
e-mail: santama@ucy.ac.cy

M. Lethan · L. B. Pedersen
Department of Biology, University of Copenhagen, Copenhagen, Denmark

M. Markaki · N. Tavernarakis
Institute of Molecular Biology and Biotechnology, Crete, Greece

C. W. Lederer
Cyprus Institute of Neurology and Genetics, Nicosia, Cyprus

S. Geimer
University of Bayreuth, Bayreuth, Germany

Introduction

Primary cilia are solitary, microtubule-based, non-motile organelles protruding from the surface of many different types of quiescent vertebrate cells or sensory neurons of invertebrates. Ciliogenesis is orchestrated by the mother centriole of the centrosome, which, upon cell cycle exit, docks to a Golgi-derived vesicle or the plasma membrane and differentiates into a basal body. In a multi-step process, the basal body then nucleates the formation and elongation

of the radial array structure of 9 + 0 microtubules (MTs) in the axoneme of the primary cilium [1–5]. Primary cilia are specialized sensory devices employing specific sets of receptors, ion channels, and transporters in the molecularly distinct membrane that surrounds them. Through these and a multitude of specific proteins in their basal body, cilia detect, transduce, and coordinate a variety of physical and chemical signals, including Hh (Hedgehog), Wnt (Wingless), PCP (planar cell polarity), and PDGF (platelet-derived growth factor) signaling, to regulate fundamental cellular processes during development and tissue homeostasis in the adult [6–9].

Considerable progress has been achieved in the elucidation of the molecular mechanisms that determine and regulate the dynamic transition between the two distinct, but intertwined, functions of centrioles: their capacity to organize MTs and assemble mitotic spindles ("centrosomal function") in cycling cells, and their ability to initiate ciliogenesis and build up the ciliary axoneme ("basal body function") [10]. For example, the functional specialization in ciliogenesis of the defining accessory structures of the mother centriole as a basal body is becoming clearer: ciliary rootlets provide mechanical support to the axoneme [11] and basal feet (or subdistal appendages) serve to anchor the cytoplasmic MTs to the base of the cilium [5, 12]. Transition fibers (or distal appendages) are involved in the connection of ciliary triplet MTs to the plasma membrane, the docking of the centriole to vesicles or the apical membrane and the creation of a diffusion barrier at the base of the cilium near the transition zone, via transport mechanisms akin to importin- and Ran-GTP-mediated nuclear import [12–15]. A growing number of basal body proteins and their interactions are now recognized for their important roles in regulating axoneme assembly or disassembly [2, 5, 16–19]. These include Bardet–Biedel syndrome (BBS) proteins, Meckel–Gruber syndrome (MKS) proteins, vesicle transport proteins Rab8, Rabin8, and Rab11, polarity proteins, protein kinases Aurora A and GSK3β, and other centrosomal/basal-body proteins, such as CP110, CEP290, CEP97, CEP164, ODF2, Chibby, and cenexin. Additionally, bidirectional intraflagellar transport (IFT) components, including anterograde kinesin-2 (KIF3A, KIF17) and retrograde dynein 2 motor proteins, and IFT-A and IFT-B complex proteins, mediating ciliary trafficking of cargo into and out of cilia, are critically important for the biogenesis and function of cilia [20–24].

By comparison, we know little about the regulatory role of MT dynamics in the cilium, which are fundamental for other MT-based cellular processes [25] and thus a likely regulator of axoneme extension and length. In cilia, MT subunits are added at ciliary tips [26] and in *Chlamydomonas,* flagellar MTs continuously turn over and require IFT for their length maintenance [27]. In mouse or human fibroblasts and retinal pigment epithelial cells MT plus end-tracking (+TIP) EB proteins, which are known to regulate the dynamics of cytoplasmic MTs [28–30], are essential for ciliogenesis and required both for MT minus end anchoring at the basal body and for regulation of axoneme length [31, 32]. In this context, new information about the involvement of different molecular chaperones, notably CCT/TRiC chaperones [33, 34], localized at cilia in diverse organisms (including *Tetrahymena, C. elegans*, and mouse), and regulating correct protein folding of tubulin, actin, and other centriolar/ciliary proteins and thus influencing ciliogenesis, is intriguing and could provide another link between axoneme dynamics and ciliary MT assembly [35–42].

Given the intimate relationship between the regulation of centriole duplication and the cell cycle, and also the tight coupling between ciliogenesis/cilium resorption and the cell cycle [43–45], it is an intriguing open question how the presence of amplified centrioles in a cell may affect ciliogenesis. In recent years, it has been demonstrated that depletion or overexpression of different centriolar and non-centriolar proteins, notably polo-like kinase Plk4, cdc kinases, AurA kinase, centriolar satellite protein CEP131, polycystin-1, BBS6, and oncoprotein E7, results in multicentrioled cells. Recent evidence suggests that cells with supernumerary centrioles can form more than one cilium, but that extra cilia often share the same ciliary pocket, with reduced ciliary concentration of signaling proteins and signaling capacity, indicating the trafficking of ciliary proteins as a rate-limiting process [46].

In earlier work, we implicated KIFC5A, a minus-end directed, mouse kinesin-14 family motor, and its interacting nucleotide-binding proteins 1 and 2 [Nubp1 and Nubp2; 47–48], in the process of centrosome duplication [49]. Depletion of KIFC5A in cultured mouse cells causes significant centriole amplification throughout the cell cycle. Supernumerary centrosomes arise as a result primarily of reduplication and partly of cytokinesis defects, contain duplicated centrioles, and have the ability to organize microtubule asters, thus leading to the formation of multipolar spindles. Nubp1 and Nubp2 interact with each other, but their individual knockdown, however, has differential effects on centrosome and spindle formation: while Nubp1 silencing qualitatively phenocopies KIFC5A silencing, also resulting in significant centrosome amplification throughout the cell cycle and the formation of multipolar spindles, Nubp2 appears to have a modulatory/accessory role for centriole arithmetics, in concert with KIFC5A and Nubp1 [49]. The Nubps, Mrp/NBP35 subclass NTPases [50], display sequence similarity with bacterial division-site-determining MinD P-loop NTPases, and are highly conserved and essential proteins throughout the Eukaryotes and have also been implicated in the assembly of cytosolic

iron-sulfur proteins and iron homeostasis in mammalian cells [51–55]. Extending our original work, we show in the present study that Nubp1 and Nubp2 are also components of the basal body and that Nubp1, Nubp2, and KIFC5A have significant effects on the capacity of cells to generate primary cilia. It is of particular interest that these three proteins appear to be involved in both aspects of centriole functionality (duplication and ciliation) and that their silencing gives the opportunity to investigate ciliogenesis in multicentriolar cells. Knockdown of KIFC5A, Nubp1, and Nubp2 thus provides a critical new tool in the ongoing investigation of the molecular mechanisms and protein interplays underlying the cilia assembly program.

Materials and methods

Cell culture

Mouse NIH 3T3 cells were cultured in DMEM (Gibco/BRL) containing 10 % v/v fetal calf serum (FCS), 2 mM glutamine, and 50 U/ml of penicillin/streptomycin, and maintained at 37 °C in 5 % CO_2. *Xenopus* XL177 epithelial cell line was cultured in L15 medium with 15 % v/v FCS, 2 mM glutamine and 50 U/ml of penicillin/streptomycin, and maintained at 25 °C in atmospheric conditions. For induction of ciliogenesis, cells were grown in serum-free media for 24 h and sampled for microscopy or Western blotting (WB) at different time points. For MT depolymerization, nocodazole (0.1 μg/ml in DMSO) or DMSO only (neg. contr.) was added to the medium for 16 h and cells were subjected to immunofluorescence (IF).

Antibodies

Antibodies against recombinant mouse Nubp1 and Nubp2, expressed as 6xHis-fusions in *E. coli* and purified by affinity-purification over Ni^{2+}-NTA beads (Qiagen), were raised in rabbits at the EMBL animal facility. Additionally, a rabbit antibody (ab) raised against 6xHis-tagged Nubp1, and a rat ab raised against 6xHis-tagged Nubp2 (each recombinant protein was affinity-purified and extracted from SDS-PAGE gels as a single band for animal injections), were generated by Eurogentec (Belgium). All abs against Nubp1 or Nubp2 were affinity-purified over CNBr-linked recombinant proteins on Sepharose 4B beads (GE Healthcare), and used at 1:300 dilution for IF and WB. A commercial mouse polyclonal anti-Nubp2 ab (Abcam ab88822; 1:100 for IF) was also employed. Anti-KIFC5A rabbit anti-peptide ab was as previously described [49]. For production of an ab against *Chlamydomonas reinhardtii* (Cr)Nubp1, cDNA was prepared [56] and the coding region of CrNubp1 (C_740040; http://genome.jgi-psf.org/chlre2/chlre2.home.html), was amplified by PCR, cloned into pMAL-c2, expressed and purified as a maltose-binding protein fusion from *E. coli* [57]. Rabbit polyclonal abs were raised against the purified recombinant protein (Yorkshire Bioscience Ltd). Additional primary and secondary abs used are listed (Table S1). Nuclei were stained with Hoechst 33342 (0.5 μg/ml).

Immunofluorescence (IF)

Cells were grown on coverslips and, depending on the primary antibody, fixed/permeabilized with methanol for 10 min at −20 °C, or fixed at room temperature with 3.7 % w/v paraformaldehyde in PHEM (30 mM HEPES, 65 mM Pipes, pH 6.9, 10 mM EGTA and 2 mM $MgCl_2$) for 10 min and permeabilized for 15 min with 0.5 % v/v Triton X-100 in PHEM. Alternatively, cells were pre-extracted for 5 s with 0.5 % v/v Triton X-100 and fixed with 3.7 % w/v paraformaldehyde in PHEM. Tracheas from wild-type adult mice were fixed in 4 % w/v paraformaldehyde in PBS overnight, embedded in paraffin, sectioned (5 μm), deparaffinized with xylene, rehydrated in a graded series of ethanol (100 to 70 % v/v), followed by distilled water, and immunolabeled. Immunolabeling in all experiments was carried out as previously described [49]. Samples were analyzed with a Zeiss Apochromat × 63 1.3 NA oil lens on a Zeiss Axiovert 200 M inverted fluorescence microscope, equipped with a Zeiss AxioCam MRm camera.

Cell-cycle synchronization and analysis under serum deprivation conditions

For synchronization of NIH 3T3 cell cultures at G1/S, a double thymidine block protocol was used [58]. Samples were collected at 2, 5, 7, 9, 12, and 14 h after release from the second thymidine block for analysis by flow cytometry and quantitative WB. For flow cytometry, harvested cells were washed in PBS, fixed with 70 % v/v ethanol, washed, stained with 1 mg/ml propidium iodide, detected on a CyFlow Cube 8 flow cytometer (Partec), and analyzed with the FCS Express 4 software (DeNovo Software), with the Multicycle AV plugin and Autofit selection. For quantification of Nubp1 and Nubp2 protein levels, intensity volumes (area × height) of protein signals on WBs (obtained with ImageJ 1.45 software) were normalized to the actin signal, run in parallel as loading control. The average of these ratios from three independent experiments, including the standard deviation (STD), were calculated and plotted. Statistical significance values were assessed by one-way ANOVA with Tukey's post test and assigned as significant [$p < 0.05$ (*)], highly significant [$p < 0.01$ (**)], or extremely significant [$p < 0.001$ (***)].

To induce cell-cycle exit and ciliogenesis, cell lines were grown in serum-free media for 24 h. Samples were collected

for WB analysis just before serum withdrawal (time point 1), after 12 and 24 h without serum (time points 2 and 3), and 12 h after serum re-introduction (time point 4). Quantification of Nubp1 and Nubp2 WB signals (four independent experiments) and statistical evaluation were as above.

Combined silencing and ciliogenesis induction protocol

Transfections with siRNAs were performed on NIH 3T3 cells using Lipofectamine 2000 (Invitrogen) and custom-made *Stealth* siRNA duplexes, specific for Nubp1, Nubp2, or KIFC5A (Invitrogen) [49] at 40 nM in the presence of serum in the transfection medium. Negative control silencing experiments were conducted in parallel with the use of "MED-GC", *medium GC content negative control* siRNA duplex (Invitrogen) [49]. Transfections were repeated 72 h after initial treatment and serum was withdrawn from the medium to induce ciliogenesis at 96 h (Fig. S7). For KIFC5A + Nubp1 double silencing, a cocktail of the two sets of siRNAs was used (20 nM of each duplex per transfection). Coverslips were harvested at 96 h just before serum withdrawal (time point 1), and at 120 h (time point 2) for (a) RNA analysis by real time RT-PCR, (b) quantitative WB to confirm depletion of target proteins, and (c) IF analysis to assess effects of silencing on centriole arithmetics and on ciliogenesis (percentage of ciliated cells). For each treatment, cells were scored for the number of centrioles, as determined by γ-tubulin or centrin staining, the count of nuclei per cell and the presence of a cilium, as visualized by double γ-tubulin (basal body) and acetylated tubulin (axoneme) labeling. The average ± STD of at least three independent experiments (total of ca. 1,000 cells per silencing condition) was determined. Statistical significance values of differences across samples were assessed by heteroscedastic and homoscedastic (as determined by the group variances) two-tailed Student's *t* tests using Microsoft Excel 2010. Overall significance of treatment effects was assessed by two-way ANOVA, followed by Bonferroni post-tests to determine the significance of differences for individual parameters (i.e., proportion of ciliated cells, proportion of multinucleated cells and number of γ-tubulin foci/cell).

Real-time RT-PCR

For relative quantification of mRNA in silencing experiments, real-time RT-PCR was conducted with the protocol and primer sequences for Nubp1, Nubp2, KIFC5A, and PBGD (calibration) described in [49].

SDS-PAGE and Western blotting

SDS-PAGE was performed using a Mini-Protean II Electrophoresis Cell (Bio-Rad) and WB was carried out with the Mini Trans-Blot Electrophoretic Transfer Cell for wet transfer (Bio-Rad), using 48 mM Tris pH 9.2, 39 mM glycine and 20 % v/v methanol as transfer buffer. Visualization of immunoreactive bands was performed with the ECL System (GE Healthcare).

Immunoprecipitation (IP) and LC–MS/MS analysis (liquid chromatography coupled with tandem mass spectrometry)

For Nubp1 IP, 20 μg of affinity-purified rabbit anti-Nubp1 ab (eluted with 100 mM glycine at pH 2.7 or pH 2.2) or rabbit IgG (neg. control) were covalently bound to Protein-A Sepharose CL-4B beads (GE Healthcare) by DNP crosslinking. Cycling NIH 3T3 cells (Fig. 8a1–a3) were lysed in TBS buffer pH 7.4, containing 0.1 % v/v Triton and 0.1 % v/v NP40. Each set of beads was incubated for 1 h at 4 °C with extracts (5 mg total protein), washed three times with lysis buffer and boiled in 100 μl of SDS-PAGE sample buffer. Forty μl from each IP was run on an SDS-PAGE gel, silver-stained and seven bands, unique to the Nubp1-IP samples, were cut out (Fig. 8a1). Bands were trypsin-digested in-gel and eluted, and tryptic peptides were separated and analyzed by LC–MS/MS (Orbitrap Velos, Thermo Scientific) at the EMBL Proteomics Core Facility. Full-scan MS spectra (mass range 300–1,700 *m/z*) were acquired in profile mode in the FT with a resolution of 30,000. Data were filtered by MaxQuant software (version 1.0.13.13) and searched in species-specific mode (mouse/human) against the Swiss-Prot database.

For CCT1 IP (Fig. 8b), the same protocol was employed, with 20 μg of affinity-purified rat anti-CCT1 ab (Table S1) or rat IgG (neg. control), covalently bound on Protein-G Sepharose 4 fast flow beads (GE Healthcare) and incubated with an extract from adult mouse brain (Fig. 8b). Bound proteins were analyzed by SDS-PAGE and WB.

C. elegans *methods*

Standard procedures for *C. elegans* were applied. A 1,110-bp region, which included the predicted promoter upstream of the operon containing Nubp1 coding sequences and which starts with gene F10G8.3 (*rae-1* gene), was amplified from genomic DNA using primers 5′cgaagcttaattcta caggaaaatattcaataaatgac3′ and 5′cgtctagatctgcaattttaattta tacagttttaaga3′, containing *HindIII* and *XbaI* sites, respectively. A 1,400-bp product, including the full-length nubp-1 coding sequences from the *C. elegans* nubp-1 gene (*WBGene00008664),* was also amplified from genomic DNA using primers 5′ggtctagaatgtctgacgtac-ctgacgacg3′ and 5′cgggatccaacaagctttgccttaactttctcag3′, containing *XbaI* and *BamHI* sites, respectively. The two fragments, joined at the *XbaI* junction, were ligated into *HindIII/BamHI* digested pPD95_77 plasmid to produce an

in-frame NUBP-1::GFP C-terminal fusion, transcriptionally driven by the copy of its endogenous promoter. To create the transgenic NUBP-1::GFP expression worm lines, this construct together with co-transformation marker pRF4 (*rol-6(su1006)*) were injected into the gonads of hermaphrodites (N2: wild-type Bristol isolate) [59]. Four independent transgenic strains were generated; the expression patterns displayed (Fig. 5) are representative of all four lines.

nubp-1 silencing experiments were carried out in *C. elegans* strain CX3553 lin-15B(n765) kyIs104 X[*lin-15*B p_{str-1}GFP, harboring GFP under the control of the *str-1* gene. The STR-1::GFP reporter fusion is specifically expressed in AWB (amphid wing B) olfactory neurons [60]. For *nubp-1* RNAi, a 1.4-kb PCR fragment that corresponds to the full-length ORF was generated using primers 5′gccgcgg atgtctgacgtacctgacgac3′ and 5′cggggcccttaaacaagctttgcc ttaac3′, containing *SacII* and *ApaI* sites and ligated into plasmid pL4440. *E. coli* strain HT115(DE3) was transformed with the above plasmid that directs the synthesis of double-stranded RNAs corresponding to the *nubp-1* gene and fed to worms for silencing, according to established methodology [61]. Animals were observed on a Zeiss LSM 710 confocal microscope, driven by Zeiss Zen software.

Culture and fractionation of ***Chlamydomonas***

C. reinhardtii strain CC-124 mt- (wild type) was grown in liquid Tris–acetate-phosphate medium [62] at 22 °C with a 14 h:10 h light:dark cycle and bubbling with air. Cells were collected by centrifugation, and resuspended in 10 mM HEPES pH 7.4; flagella were isolated by pH shock and purified by sucrose density gradient centrifugation [63]. For biochemical fractionation, freshly purified flagella were resuspended in HMDEK buffer (10 mM HEPES pH 7.4, 25 mM KCl, 5 mM $MgSO_4$, 1 mM DTT, 0.5 mM EDTA, 1 % v/v plant protease inhibitor cocktail; Sigma) containing 0.5 % v/v NP40, placed on ice for 10 min and centrifuged at 10,000×*g* for 5 min. The supernatant ("detergent extract") was collected and replaced with an equal volume of HMDEK buffer ("axonemes"). For analysis of isolated cell bodies, harvested cells were resuspended in 10 mM HEPES pH 7.4 (3×10^6 cells/ml), deflagellated by pH shock, flagella purified as above, and cell bodies treated according to Ahmed et al. [64]. Protein concentration was measured (Bio-Rad Dc assay) and samples analyzed by SDS-PAGE and WB [65].

Post-embedding immunogold electron microscopy (EM)

Small pieces of mouse trachea were fixed with 3.5 % v/v formaldehyde in 30 mM HEPES, 5 mM Na-EGTA, 15 mM KCl, pH 7.0 for 2–3 h at 4 °C and dehydrated in a graded series of ethanol. Samples were infiltrated with LR Gold resin (London Resin Company, Reading, GB) at −20 °C. Polymerization was performed under fluorescent light for 48 h at −20 °C. Ultrathin sections (60–70 nm) were cut with a diamond knife (type ultra 35°; Diatome, Biel, CH) on an EM UC6 ultramicrotome (Leica Microsystems, Wetzlar, DE) and mounted on Pioloform-coated, single-slot gold-gilded copper grids. For immunolabeling, sections were blocked for 1–2 h with blocking buffer (2 % w/v BSA, 0.1 w/v % fish gelatin and 0.05 % v/v Tween 20 in PBS; pH 7.4) and incubated with 28 µg/ml anti-Nubp1 ab in blocking buffer, overnight at 4 °C. Grids were washed with 0.15 % w/v BSA-c in PBS and incubated for 1.5 h with 12 nm gold particle conjugated-goat anti-rabbit-IgG (Jackson ImmunoResearch, Suffolk, GB), diluted 1:25 in blocking buffer. Grids were washed with 0.15 % w/v BSA-c in PBS for 10 min, postfixed for 8 min in 1 % v/v glutaraldehyde in PBS and washed in dH_2O. Sections were counterstained with uranyl acetate/lead citrate and viewed with a JEM-2100 transmission EM (JEOL, Tokyo, JP), operated at 80 kV. Micrographs were taken with a 4,080 × 4,080 pixel CCD camera (UltraScan 4000, Gatan, Pleasanton, CA, USA), driven by a Gatan Digital Micrograph software (version 1.70.16).

Results

Nucleotide-binding proteins 1 and 2 (Nubp1 and Nubp2) are stably associated with centrioles throughout the cell cycle and localize to the basal body of primary cilia in mouse cells

We initiated our analysis by probing the intracellular localization of Nubp1 and Nubp2 with the use of new, affinity purified antibodies ("Materials and methods") that each recognized a single band of the expected size in extracts from NIH 3T3 mouse fibroblasts (Fig. S1). Immunofluorescence (IF) analysis for Nubp1 in NIH 3T3 cells showed that the protein was highly enriched in centrioles at the center of MT asters at the onset of mitosis (prophase and prometaphase), and, in later mitotic phases, labeling extended locally to MTs emanating from the two asters at the two spindle poles (Fig. 1). In telophase, in addition to labeling at the poles, Nubp1 also appeared concentrated at the midbody constriction, while at interphase the protein displayed nuclear localization, excluding nucleoli (Fig. 1). The localization of Nubp2 throughout the mitotic subphases and interphase (Fig. S2A; also see Fig. 7 in [49] for initial analysis) seemed identical to that of Nubp1, an observation that was confirmed by double Nubp1 and Nubp2 co-labeling (Fig. S2, example in B). The localization patterns of Nubp1 and Nubp2 in mitosis and interphase also closely resembled that of motor protein KIFC5A [49], consistent

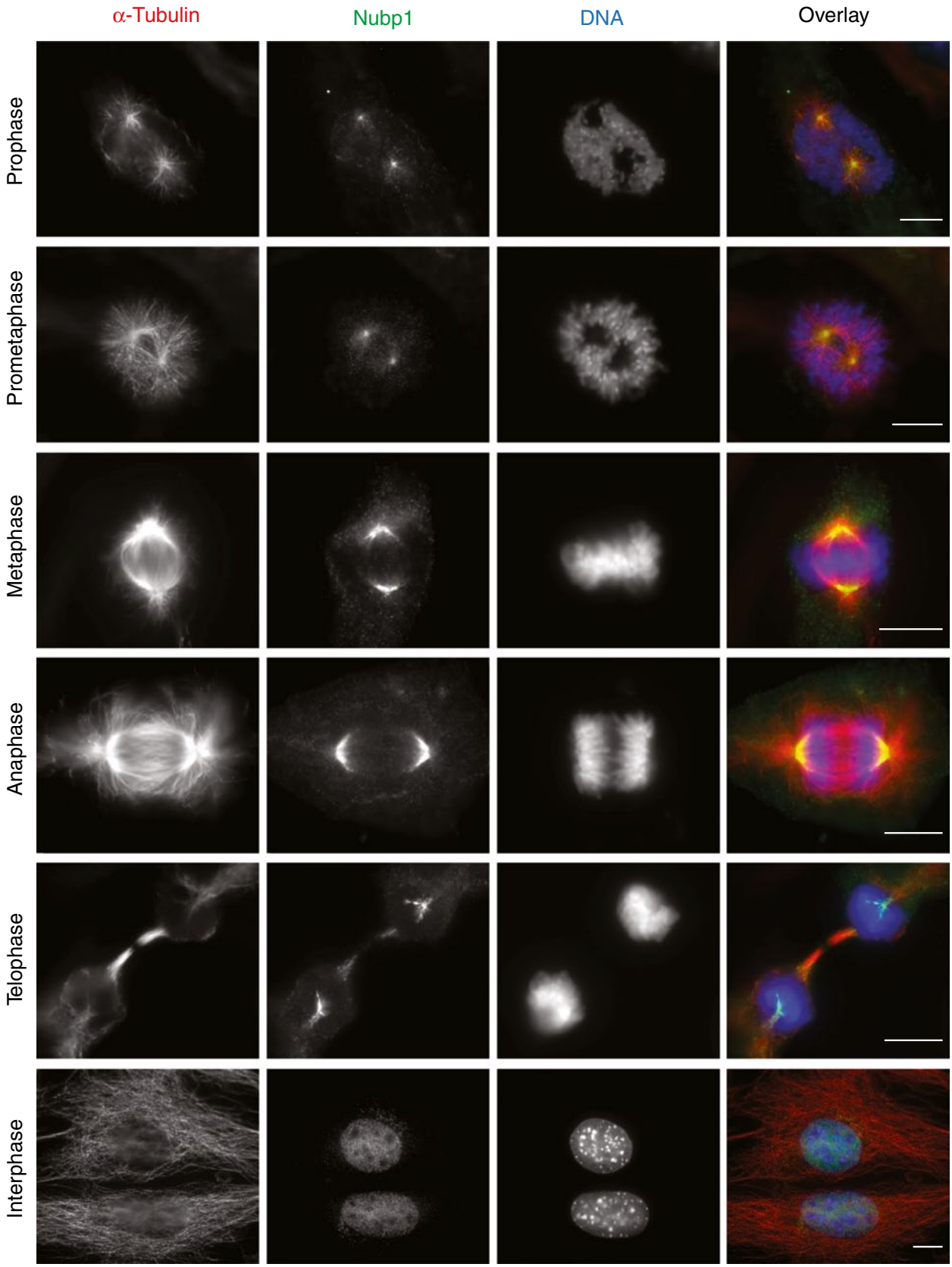

Fig. 1 Localization of Nubp1 during the phases of the cell cycle in NIH 3T3 fibroblasts. NIH 3T3 cells were processed for IF with an ab against α-tubulin (*red*) and an ab against Nubp1 (*green*). DNA was visualized with Hoechst (*blue*). *Scale bars* 10 μm

with their known interaction [49]. At interphase, however, in addition to their nuclear localization, both Nubp1 and Nubp2, but not KIFC5A, also appeared specifically associated with both centrioles of the centrosome, as revealed by double labeling with γ-tubulin, thus indicating the association of these proteins with the centrosome throughout the cell cycle (Fig. 2a1–a4 for Nubp1; c1–c4 for Nubp2; e1–e4 for KIFC5A). Nubp1 and Nubp2 appear to be integral components of centrioles since they were still detectable on centrioles following MT depolymerization with nocodazole (Fig. S3). These observations are consistent with a proteomic analysis identifying the Nubps as components of the human centrosomal proteome [66].

Because of the dual function of centrioles as the MT and spindle-organizing centers in cycling cells, and, upon cell cycle exit, the transformation of the mother centriole to the basal body, the structure that subtends a cilium, we then probed NIH 3T3 cells, induced to form primary cilia by serum deprivation ("Materials and methods"). Indeed, in serum-deprived cells that displayed a solitary primary cilium, as revealed by axonemal labeling with anti-acetylated tubulin antibody, we detected strong signals for both Nubp1 and Nubp2 (but not for KIFC5A) at the basal body, as well as in the daughter centriole that did not form a cilium (Fig. 2b1–b4 for Nubp1, d1–d4 for Nubp2, f1–f4 for KIFC5A). We obtained similar results with mouse kidney inner medullary collecting duct cells (IMCD3) (data not shown). To extend these findings, we also carried out immunogold EM on sections from mouse trachea epithelial cells, possessing characteristic arrays of multiple motile cilia, using anti-Nubp1 antibody (Fig. 3). This allowed the detailed examination of the ciliary structures: specific accumulation of gold particles was detected at the basal body itself and its appendages (ciliary roots, basal foot, and transition fibers) as well as the ciliary axoneme, including the tip and ciliary shaft. In the axoneme, labeling was predominantly localized at the periphery of the cilia in the region of the outer doublet MTs (Fig. 3a–i, panel c at high magnification). We also observed Nubp1 labeling at membrane microvilli (Fig. 3b). As the ciliary axoneme was not detectable by IF labeling for Nubp1 in primary cilia in mouse cells (Fig. 2b, d), but was detected by immunogold EM in motile cilia in mouse trachea (Fig. 3a–i) and also confirmed in motile cilia by IF of tracheal sections (Fig. S4), this was indicative of a great difference in the axonemal enrichment for Nubp1 in primary vs. motile cilia.

Finally, given the pair-wise interactions between KIFC5A, Nubp1, and Nubp2, we examined whether the association of each of the proteins with centrioles at mitosis or interphase, or with the basal body at quiescence, was dependent on the presence of the other two proteins. When we silenced KIFC5A, we could detect both Nubp1 and Nubp2 in all of the amplified centrioles (the hallmark of KIFC5A silencing; [49]) at mitosis and interphase, excluding the possibility that KIFC5A is the motor protein responsible for their centriolar translocation (Fig S5 A1-D3). Likewise, depletion of Nubp1 or Nubp2 did not appear to affect the localization of the respective other proteins on centrioles or the basal body (Fig. S5, E1-F3 and data not shown), indicating their independent recruitment.

The association of Nubp1 with basal bodies and cilia is phylogenetically conserved

We next investigated whether the association of the Nubp proteins with the cilium was of more general significance and thus studied cells and organisms representing disparate phyla. First, we noticed that our anti-Nubp1 antibody, raised against mouse Nubp1, seemed to also work efficiently and specifically in *Xenopus* cells, presumably recognizing the native Nubp1 protein (xNubp1), given that the pattern of IF obtained in the XL177 epithelial-derived cell line of *Xenopus* was equivalent to what we had documented in mouse cells (Fig. S6). Upon serum deprivation, like in mouse cells, there was distinct Nubp1 labeling of the basal body of the single primary cilium in *Xenopus* XL177 cells (Fig. S6 bottom panels).

Proteomic analysis of isolated *C. reinhardtii* flagella had indicated that a homolog of Nubp1 (CrNubp1) is present in flagella, albeit at low abundance [67]. To confirm this, we generated an antibody against CrNubp1 ("Materials and methods"), which detected a single band of ca. 50 kDa in WB analysis of isolated flagella (Fig. 4a), slightly higher than the predicted molecular mass of CrNubp1 (40.6 kDa). This discrepancy is likely due to the acidic nature of CrNubp1 (p$I = 4.95$), which could cause abnormal migration in SDS-PAGE. The CrNubp1 band appeared enriched in flagella compared to cell bodies, similar to the IFT-A protein IFT139 (Fig. 4b; note that despite maximum protein load, the CrNubp1 band was not detectable in purified cell bodies). Biochemical analysis indicated that CrNubp1 primarily associates with the flagellar axoneme although some is present in the detergent-extractable membrane and matrix fraction, similar to EB1 (Fig. 4c). CrNubp1 did not appear to co-fractionate with the flagellar kinesin-14 motor protein KCBP [68] (Fig. 4c), and we also failed to detect association between these two proteins using pull-down assays or IP (data not shown).

We also generated four strains of *C. elegans* that expressed a construct containing the *C. elegans* Nubp1 orthologue (NUBP-1), C-terminally fused with GFP and driven by a copy of its innate promoter. This enabled us to observe NUBP-1 expression in the whole animal and revealed that, although not uniquely confined at this site, NUBP-1::GFP accumulation was prominent and consistent in clusters of ciliated sensory neurons at the head of the

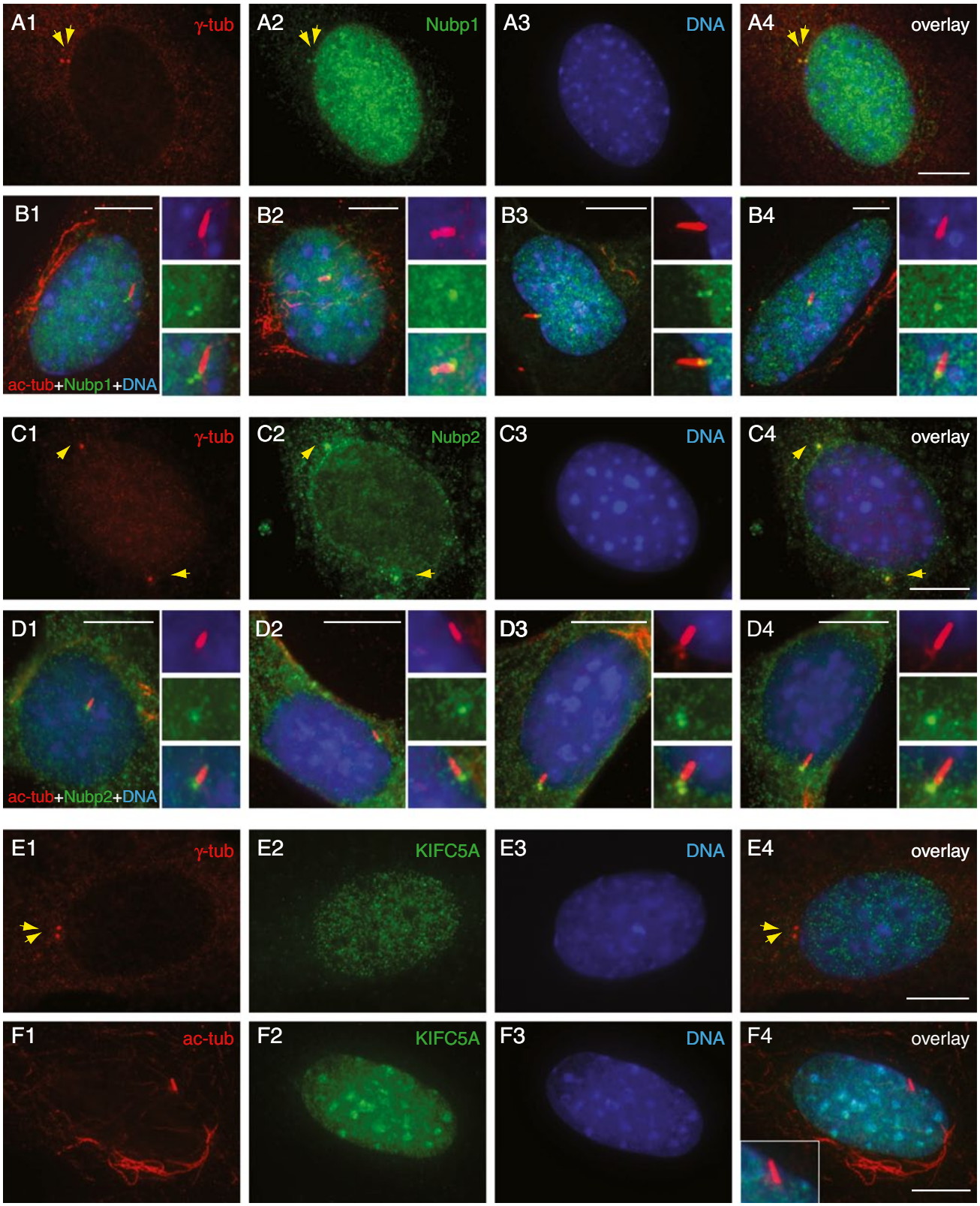

animal (amphid and labial neurons; Fig. 5a1–a3) and ciliated chemosensory neurons at the tail (phasmid neurons; Fig. 5b1–b2). All are well-characterized sensory neurons involved in chemo-, thermo-, osmo-, or mechano-sensation and extend dendrites with non-motile ciliated endings (sensilla) [69–72].

◀ **Fig. 2** Nubp1 and Nubp2, but not KIFC5A, localize on interphase centrioles in cycling cells and basal bodies in quiescent cells. **a1**–**a4** Immunostaining of NIH 3T3 mouse fibroblasts, using abs against γ-tubulin (*red* **a1**), Nubp1 (*green* **a2**) and counterstaining for DNA (*blue* **a3**), indicates the presence of Nubp1 on centrioles (*yellow arrowheads*). Overlay shown in **a4**. **b1**–**b4** Series of examples of localization of Nubp1 at the basal body of primary cilia in serum-deprived NIH 3T3 fibroblasts. Shown is the overlay of acetylated tubulin (as a ciliary axoneme marker; *red*), Nubp1 labeling (*green*) and DNA labeling (*blue*) in the larger image of each set. Magnified views of the cilium appear in the accompanying three smaller images. (In addition to the primary cilium axoneme, acetylated tubulin-containing MTs are visible in some cells, the presence of which is well documented in current literature, as reviewed by [102, 103]). **c1**–**c4** Immunostaining of γ-tubulin (*red* **c1**), Nubp2 (*green* **c2**) and counterstaining for DNA (*blue* **c3**) also shows localization of Nubp2 on centrioles (*yellow arrowheads*). Overlay shown in **c4**. **d1**–**d4**. Series of examples of localization of Nubp2 at the basal body of primary cilia in serum-deprived NIH 3T3 fibroblasts, showing acetylated tubulin (*red*), Nubp2 labeling (*green*) and DNA labeling (*blue*) and accompanying magnified views of the cilium. **e1**–**e4** In contrast, immunostaining using abs for γ-tubulin (*red* **e1**), KIFC5A (*green* **e2**), and counterstaining for DNA (*blue* **e3**) indicates the lack of KIFCF5A from interphase centrioles. Overlay shown in **e4**. **f1**–**f4** Series of examples to indicate lack of basal body localization of KIFC5A; acetylated tubulin (*red*), KIFC5A labeling (*green*), and DNA labeling (*blue*). *Scale bars* 10 μm; details in the accompanying small images are shown at double the magnification of their corresponding main image

Taken together, these results revealed a remarkably conserved localization of Nubp1 in both motile and non-motile cilia in phylogenetically distant organisms, spanning unicellular and multicellular invertebrate and vertebrate Eukaryotes.

Depletion of Nubp1 or Nubp2 affects cilium morphology and significantly increases the ability of cultured cells to form primary cilia

The intriguing localization and phylogenetic conservation of the Nubp proteins on basal bodies of both non-motile cilia (mouse primary cilia, *C. elegans*) and motile cilia (mouse trachea, *Chlamydomonas*), prompted us to investigate the functional relationship of Nubp1 and Nubp2 with the formation of cilia. First, we conducted RNAi for *nubp-1* over a marker strain of *C. elegans* that expresses GFP driven by the promoter the *str-1* gene, encoding a G protein-coupled seven-transmembrane receptor protein, which uniquely labels the ciliated AWB (amphid wing B) olfactory amphid neurons [60]. Strikingly, NUBP-1 depletion resulted in abnormal cilia morphology in silenced AWB neurons, compared to control silencing (Fig. 5c–d3; from a typical "two-pronged fork" shaped cilia of AWB in control cells to "winged-like" structures in *nubp-1*-silenced cells) and even the presence of additional dendritic ciliated endings than the normal two per neuron (Fig. 5d3, extra cilium indicated by *red arrow*). These results indicated the involvement of NUBP-1 in the process of ciliogenesis by regulating cilium structure and/or suppressing cilium formation.

To extend the *C. elegans* results, we next performed a series of silencing experiments in NIH 3T3 cells. In earlier work, we had documented that siRNA-mediated depletion of KIFC5A in NIH 3T3 cells caused significant centriole amplification throughout the cell cycle, formation of multipolar spindles and an increase of the incidence of multinucleated cells. Further, we reported that silencing of Nubp1 qualitatively phenocopied the KIFC5A silencing effect, while silencing of Nubp2 alone caused no centrosome amplification and no discernible anomaly in spindle organization but Nubp1/Nubp2 co-silencing quantitatively augmented centriole amplification, compared with single Nubp1 or KIFC5A silencing, suggesting a modulatory/accessory role for Nubp2 in concert with KIFC5A and Nubp1 [49]. Here we adapted our original protocol to include an additional step of 24-h serum deprivation to induce ciliogenesis, after silencing had been applied to maximum effect, which would thus allow us to examine possible effects of depletion of each of the proteins on cilia formation. In our protocol (Fig. S7A), cell sampling took place at 96 h (just before serum deprivation) as a reference point for silencing in cycling cells, without induction of ciliogenesis, and at 120 h as a point to assess ciliogenesis in the absence of the depleted protein(s) under study in quiescent cells. Using an antibody to proliferation marker Ki67, robust expression was displayed by cells harvested at 96 h (Fig. S7B1–B2), while the lack of Ki67 signal in cells at 120 h (Fig. S7C1–C2; in C2 same exposure as in B2) and high incidence of primary cilia (Fig. S7D) indicated cell-cycle exit and induction of ciliogenesis. Silencing was confirmed by real-time RT-PCR (data not shown), quantitative WB with the appropriate antibody against the silenced protein(s) in each case (Fig. 6a–c) and quantitative verification of the previously established phenotypes of centriole amplification and increase of multi-nucleated cycling cells (Fig. S8).

Having confirmed the efficacy of the silencing protocol and having successfully reproduced the previously characterized effects of silencing on centriole arithmetics, we proceeded, in the same samples, to examine the effect of the knockdown of each of the proteins on ciliogenesis by microscopically scoring the number of ciliated cells, as revealed by double γ-tubulin/acetylated tubulin labeling, in each of the silenced and control populations. We compiled large scoring datasets (1,000 silenced and 1,000 control-silenced cells per silencing regime) and observed that cultures subjected to KIFC5A silencing and serum deprivation (time point 120 h) had a markedly reduced ability of ciliogenesis, resulting in a decreased number of ciliated cells. In particular, the average percentage of ciliated cells in the KIFC5A-silenced population was only 50.53 % of the

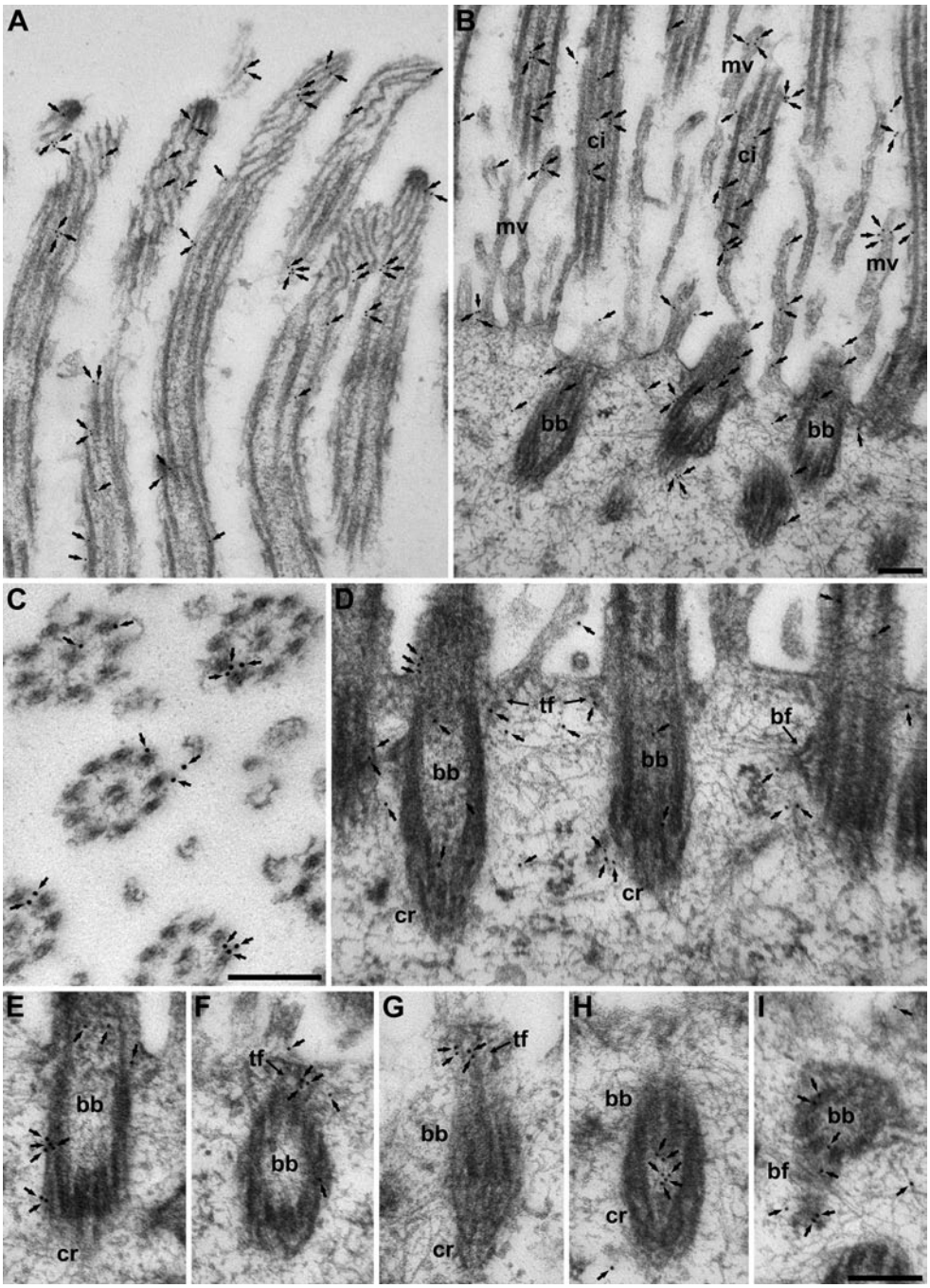

Fig. 3 Nubp1 is localized on motile cilia and their basal bodies by immunogold EM. Postembedding immunogold labeling of mouse tracheal epithelial cells with anti-Nubp1 ab showing ciliary (**a**–**c**) and basal body (**b**, **d**–**i**) Nubp1 localization. All individual gold particles are indicated with *arrows* for easier identification. **a** Longitudinal section of the distal parts and ciliary tips of a group of cilia. Ciliary shafts and tips are labeled with gold particles. **b** Longitudinal section of basal bodies, proximal parts of cilia and microvilli. Nubp1 labeling is found at the basal bodies (bb), cilia (ci) and microvilli (mv). **c** Cross section (slightly oblique) of a group of cilia. Gold particles are predominantly found at the periphery of the cilia in the region of the outer doublet MTs/ciliary membrane. **d** Longitudinal section of a group of basal bodies. Gold particles can be found at the bb, ciliary roots (cr), and transitional fibers (tf) interconnecting the bb with the plasma membrane. A network of fibers surrounding the bb, some of which are attached to the basal feet (bf), is also labeled. **e** Slightly oblique longitudinal section of a bb grazing the cr. Gold particles are visible in a median and proximal position at the bb, likely representing attachment sites of filaments of the cr. **f** Oblique longitudinal section of a bb with Nubp1 labeling at the tf. **g** Grazing longitudinal section of a bb and cr. Gold particles are associated with the tf. **h** Oblique longitudinal section of the proximal end of a bb and associated cr showing Nubp1 labeling. **i** Oblique cross section of a bb and associated bf, labeled with gold particles. *Scale bars* 200 nm (*bar* shown in **b** applies to images **a** and **b**; *bar* in **i** applies to **d**–**i**)

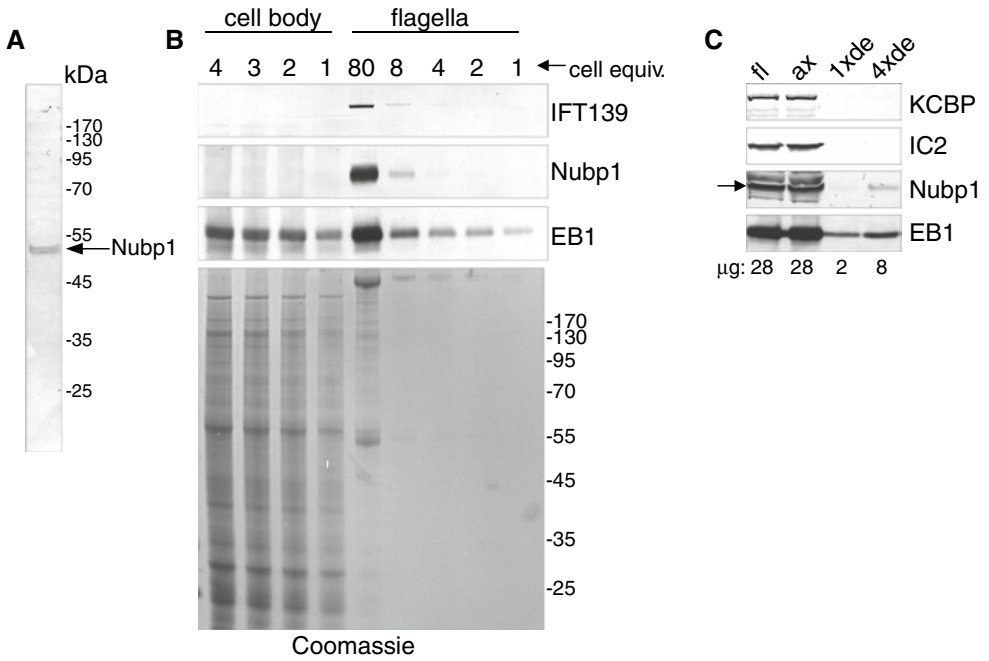

Fig. 4 A Nubp1 homolog is present in *C. reinhardtii* flagella. **a**–**b** WB analysis with CrNubp1 ab detected a single band of ca. 50 kDa in isolated *C. reinhardtii* flagella (**a**). In **b**, different amounts of isolated cell bodies and flagella were subjected to WB analysis with the antibodies indicated (*top panels*). A gel run in parallel was stained with Coomassie blue (*bottom panel*). *Numbers above the lanes* correspond to the relative amount ("cell equiv.") loaded in each lane. CrNubp1 appears enriched in flagella, similar to IFT139, whereas EB1 is more abundant in cell bodies. Note that we could not detect CrNubp1 in cell body extracts, despite maximum protein load. **c** Freshly prepared flagella (fl) were extracted with non-ionic detergent ("Materials and methods") and the axonemal fraction (ax) and an equivalent (1xde) or fourfold larger volume (4xde) of detergent extract were analyzed by SDS-PAGE and WB with the antibodies indicated. The corresponding amounts of proteins (in µg), loaded per lane, are shown at the *bottom*. CrNubp1 is present on isolated axonemes with a small fraction of Nubp1 being detected in the detergent soluble membrane-matrix fraction

average of control-silenced levels [11.26 ± 5.33 % (SD) in KIFC5A silencing vs. 22.28 ± 4.46 % in control silencing] and was statistically highly significantly different (six independent experiments, $p = 0.003$) (Fig. 6d). On the contrary, either Nubp1 or Nubp2-silenced cells displayed a strikingly augmented ability to form cilia, compared to controls, resulting in significantly increased percentages of ciliated cells. In particular, the average percentage of ciliated cells in Nubp1 silencing was increased by 68.86 % compared to control silencing [36.77 ± 5.21 % in Nubp1 silencing vs. 21.78 ± 3.42 % in control silencing] (six independent experiments, $p = 0.00015$) (Fig. 6e). Similarly, the increase in Nubp2-silenced cells was 96.78 % of control-silenced levels [34.27 ± 10.17 % in Nubp2 silencing vs. 17.42 ± 5.52 % in control silencing] (six independent experiments, $p = 0.0051$) (Fig. 6f). Similar trends were observed in the 96-h samples and maintained their statistical significance, although the absolute values of the average percentages were low, owing to the small number of ciliated cells in the presence of serum (Fig. 6d–f).

Intriguingly, when we applied double silencing for KIFC5A and Nubp1, we observed no noticeable difference between the percentage of ciliated cells in silenced and control-silenced populations either at 120 or at 96 h (at 120 h 28.21 ± 2.07 % in KIFC5A + Nubp1 double silencing vs. 25.15 ± 8.56 % in control silencing, $p = 0.43$), as if the opposing influences of KIFC5A and Nubp1 in ciliogenesis had balanced each other out (Fig. 6g). However, the high incident of multinucleated cells observed for individual KIFC5A silencing and, to a lesser extent, Nubp1 silencing, was strongly maintained in double-silenced cells at 120 h (higher by an order of magnitude vs. control cells) and was statistically highly and extremely significant in 96- and 120-h populations, respectively (Fig. S9A2). This was not the case anymore with the average number of centrioles per cell, which was comparable in silenced and control populations (Fig. S9A1). The partial divergence of individual and combined silencing phenotypes, namely the maintenance of individual effects upon co-silencing in cycling cells and their canceling-out with regard to ciliogenesis, indicated a multifaceted action of these proteins.

Since depletion of Nubp1 or Nubp2 increases ciliation frequency in NIH 3T3 cells (Fig. 6), we next investigated their relative protein levels throughout the cell cycle and upon serum deprivation/induction of ciliogenesis in NIH 3T3 cells. First, we used a G1/S cell-cycle

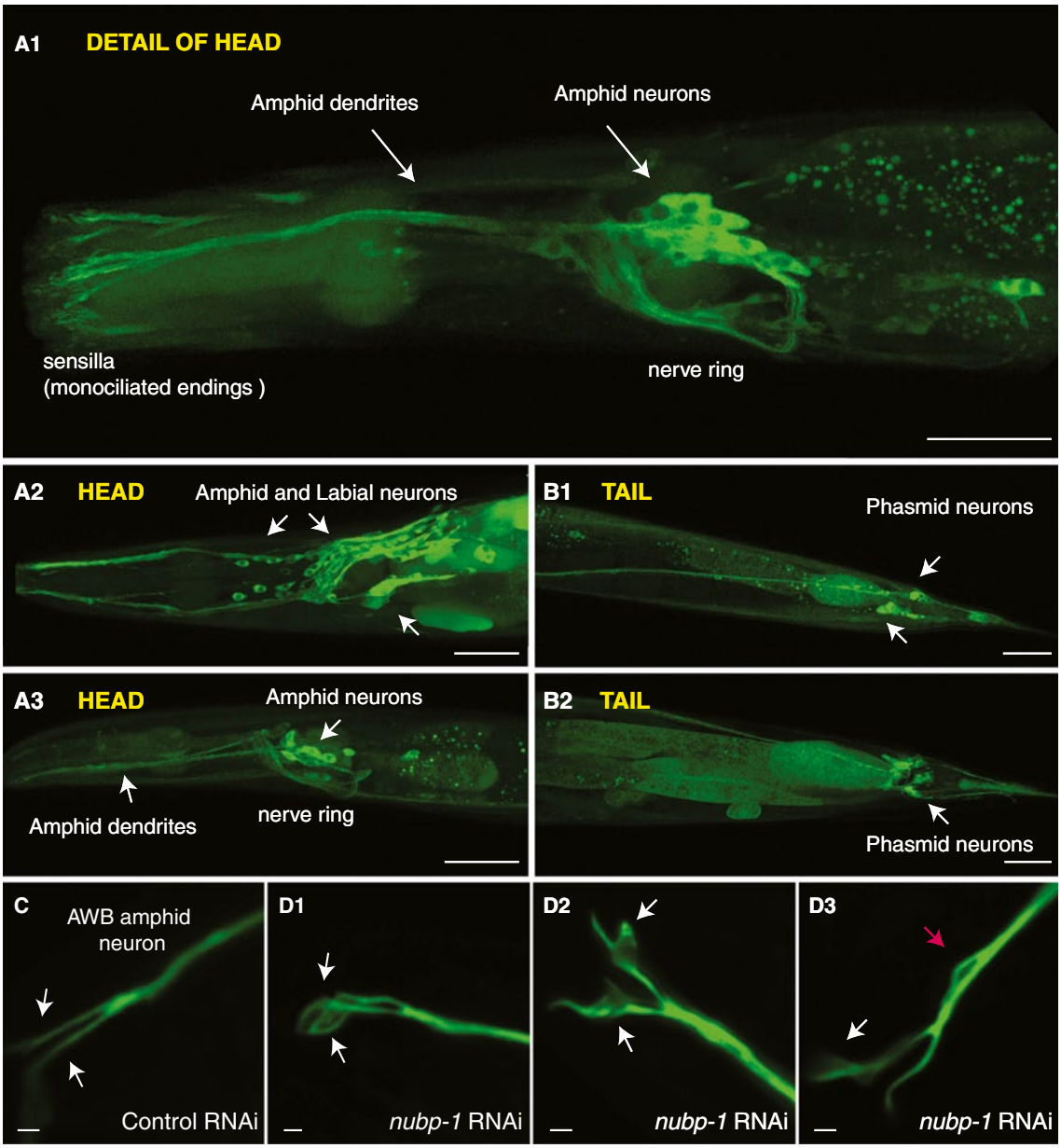

Fig. 5 In *C. elegans*, NUBP-1 is highly expressed in ciliated cells and its downregulation causes abnormal cilia morphology and number. **a1**–**b2** Maximal projection reconstruction of confocal images of representative examples at the head and tail of a *C. elegans* strain, expressing NUBP-1::1-GFP under transcriptional control of the promoter driving expression of the endogenous *nubp-1* gene. Prominent sites of localization, as indicated by GFP fluorescence, were identifiable groups of ciliated amphid and labial neurons in the head and phasmid neurons in the tail. *Scale bars* 30 μm. **c**–**d3** Details of AWB (Amphid Wing B) olfactory neurons, with their ciliated endings (*arrowheads*), specifically expressing $p_{str\text{-}1}$GFP reporter fusion, that allows their definitive identification. Silencing of *nubp-1* in this strain results in clear disruption of cilia morphology (examples in panels **d1**–**d3**), compared to control silencing (**c**). In panel **d3**, the *red arrow* points to an abnormal additional (third) cilium. *Scale bars* 1 μm

synchronization protocol, followed by biochemical analysis (SDS-PAGE and quantitative WB) and statistical evaluation. We achieved efficient cell synchronization [FACS analysis (data not shown) and use of the mitotic marker dimethylated/phosphorylated histone H3 (Fig. S10A1–A2)], and observed constant Nubp1 and Nubp2 protein levels throughout the cell cycle (Fig. S10B1–C2). On the contrary, analysis of Nubp1 and Nubp2 levels during growth (first time point), serum starvation (two subsequent time points) and serum re-introduction (last time point) revealed a significant decrease of both Nubp1 and Nubp2 levels during cell-cycle exit and also a trend to re-increase rapidly towards previous levels after serum re-introduction (Fig. S11). These results, revealing stable levels of Nubp1

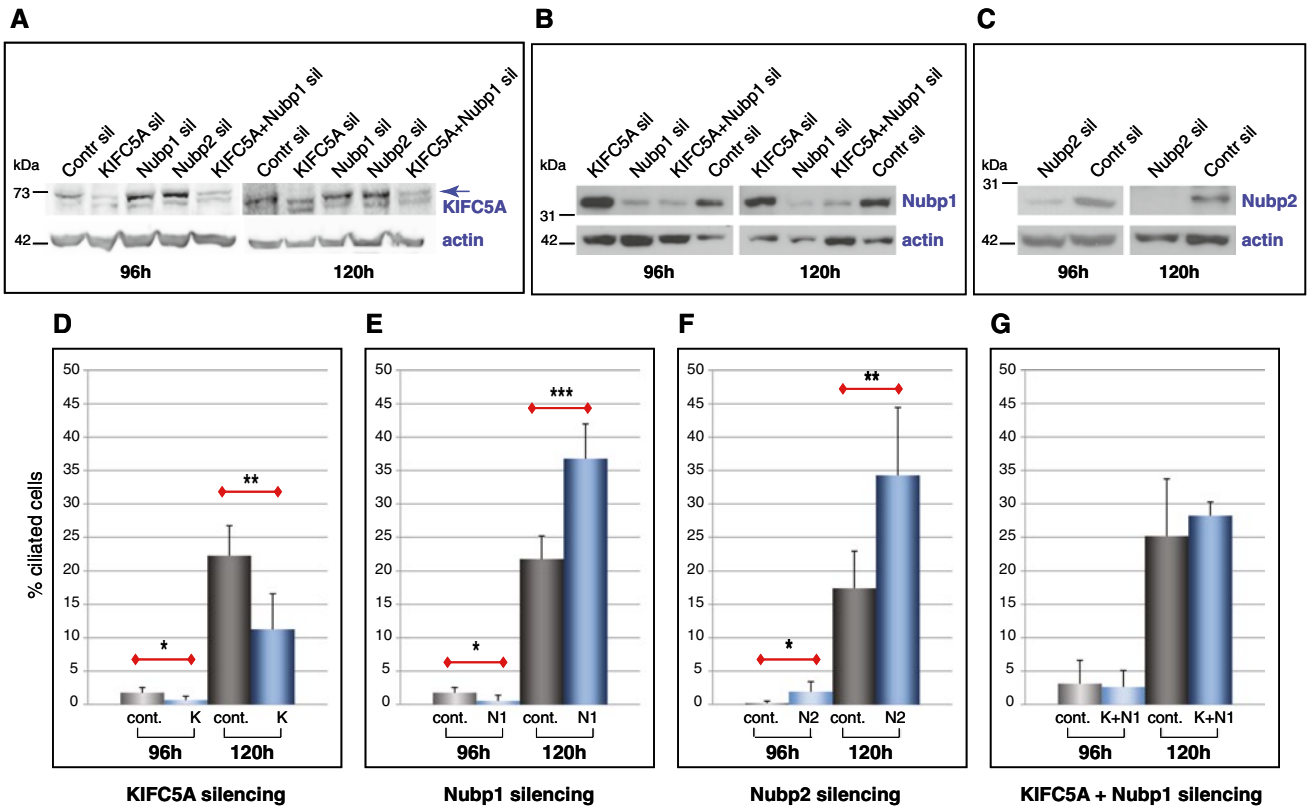

Fig. 6 Silencing of KIFC5A, Nubp1, or Nubp2 influences the ability of cells to generate primary cilia in mouse NIH 3T3 cells. **a–c** Representative WB to confirm single or double silencing, using appropriate antibodies in each case (as indicated; the KIFC5A band is pointed at by an *arrow* and is sometimes accompanied by a closely migrating *lower band*). The concurrent detection of actin was used as a loading control and the actin signal was used to normalize signal intensities for other protein, as detailed in "Materials and methods". **d–g** Quantification of the percentage of ciliated cells in KIFC5A-, Nubp1-, Nubp2-, or double KIFC5A + Nubp1-silenced populations, compared with corresponding control-silenced populations, at 96 h (growth conditions) and after induction of ciliogenesis by serum deprivation at 120 h (cell cycle arrest). Shown are the averages from four independent experiments. *Bars* represent standard deviation (STD) values. Differences are significant (*), very significant (**), or extremely significant (***), as indicated. *Cont.* control silencing, *K* KIFC5A-, *N1* Nubp1-, *N2* Nubp2-silencing

and Nubp2 in cycling cells and reduced levels during ciliogenesis, are in line with the idea that Nubp1 and Nubp2 may be acting as negative regulators, keeping ciliogenesis at bay in the cell cycle; their downregulation in quiescence coincides with increased ciliogenesis, similar to the effects obtained with silencing of each of the proteins (Fig. 6).

Basal bodies and centrioles mature normally in silenced cells lacking Nubp1 or Nubp2

We sought to address the mechanisms through which Nubp1 and Nubp2 affect ciliogenesis and the question of why depletion of Nubp1 seemed to facilitate ciliogenesis while the contrary was the case for KIFC5A, given that a landmark of the phenotypes induced by the lack of each of the two proteins was the same, i.e., significant centriole amplification. By detailed qualitative analysis of the silencing datasets, we noticed that, despite the large overall difference in the incidence of ciliogenesis (Table 1a), there was no notable difference in the relative percentages of multicentriolar cells within the ciliated cell population compared to the non-ciliated cell population (Table 1e, f). In addition, for each silencing regime and within the subpopulation of multicentrioled cells, the percentage of cells that were able to form a cilium was similar to that of ciliated cells with two centrioles but differed between the two groups (Table 1c, d, e). From these findings, we conclude that (a) centriole amplification per se was not an impediment to the ability of a cell to support ciliogenesis as effectively as two-centrioled cells (i.e., by competing for and diluting out of factors essential for ciliogenesis), (b) compared to KIFC5A-silenced multicentrioled cells, Nubp1-silenced multicentriolar cells appeared more potent in their ability to initiate ciliogenesis. This was similar to their two-centrioled counterparts, compared to two-centrioled KIFC5A-silenced cells. It therefore appears

Table 1 Quantification of ciliogenesis in mouse NIH 3T3 cells possessing two or multiple centrioles, under KIFC5A-, Nubp1-, or control-silencing regimes

	Silencing regime	KIFC5A	Nubp1	Control
a	% of total ciliated cells in population	11.26 ± 5.33	36.77 ± 5.21	22.28 ± 4.46
b	% of total multicentrioled cells in population	7.24 ± 2.33	5.88 ± 1.65	1.64 ± 0.86
c	% of ciliated cells within multicentrioled population	9.04 ± 8.20	46.43 ± 10.58	12.50 ± 12.50
d	% of ciliated cells within population with two centrioles	11.41 ± 5.13	36.26 ± 2.25	22.43 ± 3.99
e	% of multicentrioled cells within ciliated cell population	6.90 ± 7.46	7.17 ± 1.27	0.92 ± 0.82
f	% of multicentrioled cells within non-ciliated cell population	7.36 ± 2.26	5.14 ± 2.17	1.82 ± 0.94

that the ciliogenesis potential in each case was inherent to the centrioles formed under each of the silencing regimes and in the absence of the corresponding proteins. Interestingly, we observed rare instances where multicentrioled cells possessed two cilia, organized by distinct basal bodies (examples in Fig. 7 and S13). Similarly, although also rare, we observed multinucleated cells with two or more centrioles with fully formed cilia in both Nubp1 and KIFC5A silencing. Indeed, both quantitative results above, taken together with the differential effects of the different silencing regimes on ciliogenesis and centriole duplication, lend support to the hypothesis that the impact of Nubp1, Nubp2, and KIFC5A on the two processes is mediated by distinct pathways.

On this background, we therefore inquired whether the compositional modifications required for a centriole to transform to a basal body, as a pre-requisite for ciliogenesis, may have been influenced by depletion of the Nubps or KIFC5A. The distal end of the mother centriole functions as the site of the initiation of the cilium in quiescent cells and distal-appendage specific components are found to be essential for ciliary axoneme assembly ("Introduction"). The protein Chibby (Cby), a distal-end component of mother centrioles and an antagonist of the Wnt/β-catenin signaling pathway [73], is essential for the organization of both primary and motile cilia in mouse, in collaboration with its interacting protein cenexin (cnx), a distal/subdistal appendage and also mother centriole-specific protein [74]. Cycling cells display one Cby-labeled centriole, corresponding to the mother centriole, or one Cby dot per centriole pair, following centrosome duplication and at the onset of mitosis; in ciliated cells Cby uniquely associates with the basal body at the base of the cilium [74]. In all cases, the Cby dot appears peripheral to centriole markers such as γ-tubulin or centrin [74]. We observed exactly this characteristic pattern of unique association of mother centriole/basal body Cby localization in control-silenced cycling cells at 96 h and ciliated quiescent cells at 120 h (Fig. 7a, b, respectively). On the contrary, in KIFC5A-, Nubp1-, and Nubp2-silenced cells at 96 h, possessing two or more centrioles (as a result of amplification and cytokinesis defects, [49]) we consistently observed that both centrioles (when the cell had two centrioles), or more than half and up to, sometimes, all of the centrioles (when the cell had several amplified centrioles), displayed Cby labeling (Fig. 7c–h for several examples and other data not shown). This indicated that there was likely no failure in the maturation process of amplified centrioles, assembled in the absence of KIFC5A, Nubp1, or Nubp2, and that centrioles were randomly sorted to daughter cells resulting in cells that possessed several mature centrioles that could potentially become basal bodies. In silenced cells at 120 h, Cby was always detected in the basal body that formed a cilium, regardless of whether the cell had multiple other (two or more) Cby-bearing centrioles and this observation was the same for KIFC5A, Nubp1, or Nubp2-silenced populations (Fig. 7i, m, n and data not shown). This suggested that Cby was essential for axoneme formation (in line with published work) and also indicated that the presence of multiple mature mother centrioles in the same cell is not per se inhibitory for primary cilia formation. In fact, we observed instances of cells with two cilia emanating from the two Cby-positive centrioles present, or from two of several Cby-positive centrioles in the same cell (Fig. 7j, k, o). Finally, although essential, the presence of Cby was not sufficient to initiate ciliogenesis because we documented examples of Nubp1- and KIFC5A-silenced cells with amplified, Cby-containing centrioles that were unable to form cilia (Fig. 7l, p). Consistent with our results on Cby localization, we confirmed that Cnx, required upstream for recruitment of Cby to mother centrioles, was also present in multiple centrioles at 96 h and was always part of the basal body organizing the cilium at 120 h (Fig. S12).

We also examined distal end proteins CP110 and CEP290 (Fig. S13). The dual function of CP110 is important both for the regulation of centriole duplication and for suppression of the ciliogenesis program in cycling cells [16, 75, 76]. CP110 interacts with Cyclin F and is an

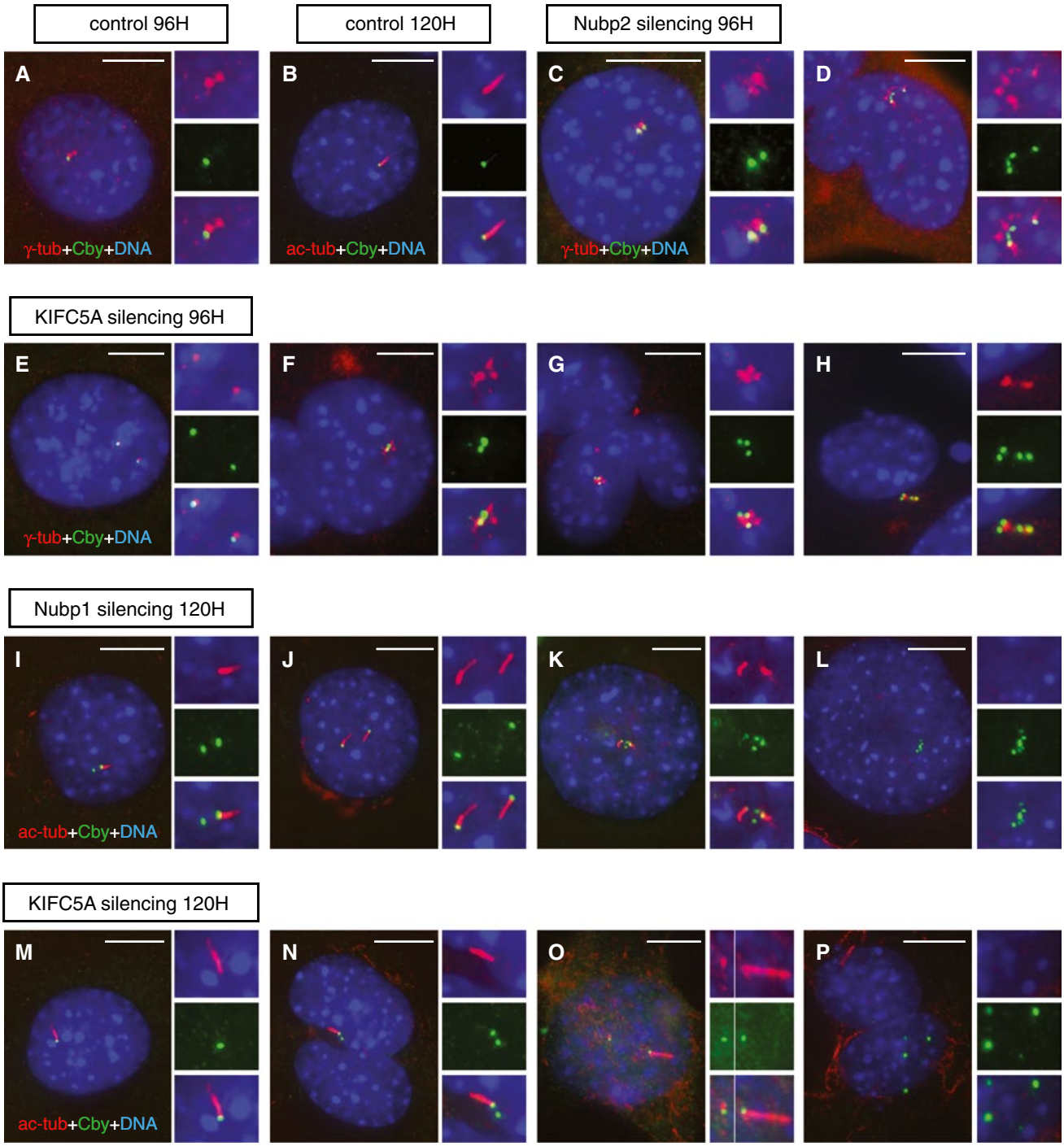

Fig. 7 Recruitment of Chibby in amplified centrioles and the basal body in silenced mouse NIH 3T3 cells. **a**–**b** Chibby (Cby) localizes only to the mother centriole in control-silenced cycling cells (96 h; panel **a**) and to the basal body in serum-deprived cells (120 h; panel **b**), as revealed, respectively, by double labeling for γ-tubulin (*red*) and Chibby (*green*) or acetylated tubulin (*red*) and Chibby (*green*). DNA counterstaining (*blue*). **c**–**h** On the contrary, Chibby is found in many, and sometimes all, of the amplified centrioles in silenced cycling cells at 96 h. Examples of Nubp2-silenced cells (panels **c** and **d**) or KIFC5A-silenced cells (panels **e**–**h**), as shown by double labeling for γ-tubulin (*red*) and Chibby (*green*) and DNA counterstaining (*blue*). **i**–**p** In serum-deprived ciliated cells at 120 h of silencing, Chibby is maintained not only at the basal body of the cilium but also in many, or even all, of the additional centrioles. Series of examples in Nubp1-silenced cells (panels **i**–**l**) and KIFC5A-silenced cells (panels **m**–**p**), as revealed by double staining for acetylated tubulin (*red*) and Chibby (*green*) and DNA counterstaining (*blue*). *Scale bars* 10 μm; details in the accompanying small images are shown at double the magnification of their corresponding main image

ubiquitination substrate of the $SCP^{cyclinF}$ ubiquitin ligase, which mediates its degradation, thought to be required for ciliogenesis to proceed [16, 58]. CEP290, which forms complexes with CP110, seems to have a ciliogenesis-specific function by regulating the appropriate localization of Rab8 to centrioles and basal bodies [17, 18]. Here, both CP110 and CEP290 localized appropriately to centrioles and basal bodies in Nubp1, Nubp2 and KIFC5A-silenced cells at 96 and 120 h, similar to control-silenced cells (Fig. S13). Supernumerary amplified centrioles arising from Nubp1- or KIFC5A-depletion retained CP110 and CEP290, suggesting that they could be subject to the normal mechanisms of regulation in cycling or quiescent cells. Consistent with this notion, we observed a decrease in CP110 signal intensity at the basal body of ciliated cells, relative to the accompanying daughter centriole, as would be expected and similar to control-silenced cells (Fig. S13B1–B4).

We analyzed other ciliary proteins, crucial to the process of ciliogenesis, namely the CP110/CEP290-interacting small GTPase Rab8, required for the biogenesis of ciliary membrane [77–79], AurA protein kinase, involved in the regulation of ciliary disassembly [19], and centrin 2, an integral EF-hand Ca^{2+}-binding centriolar protein required for centriole duplication [80]. In all cases, we found the proteins appropriately recruited to centrioles/basal body in all silencing regimes, including double silencing of Nubp1 + KIFC5A (Fig. S14 and data not shown).

Overall, therefore, we conclude that basal bodies mature normally and the observed effects of silencing of the interacting proteins Nubp1, Nubp2 and KIFC5A on ciliogenesis do not result from lack of recruitment of some key factors influencing the formation of primary cilia.

Nubp1 interacts with several members of the TCP1/CCT chaperone-containing complex

To understand the molecular basis of the involvement of the Nubps in ciliogenesis, we performed IP experiments using our anti-Nubp1 antibody (two different batches of affinity-purified antibody, eluted at different pH). We isolated seven protein bands that were uniquely identified in the Nubp1-IP complexes and lacking from the negative control IP (Fig. 8a1) and subjected them to MS identification. Band no. 4 contained Nubp1, as expected from its size/migration pattern and immunoreactivity to the Nubp1 antibody (Fig. 8a1–a2), and bands no. 2 and 3 were identified as containing several subunits of the TCP1/CCT chaperone complex, namely CCT subunits γ, δ, ε, ζ, η, θ (or CCT3-CCT8). Table S2 lists all the proteins identified in the 7 isolated bands. CCT/TRiC chaperone family complex is an eight-subunit, evolutionarily conserved 900-kDa cylindrical structure that can internalize other proteins into its central cavity, composed of two octameric rings, and promote their folding in an ATP-dependent manner [81]. Tubulin and actin were originally identified as its substrates, underlining the importance of the chaperonin complex in cytoskeleton maintenance [82], however today it is understood that the CCT mediates proper folding of a broad spectrum of proteins [83–85] and also promotes the activation of the APC (anaphase promoting complex), thus serving an essential function in cell-cycle progression [86]. In addition to being cytoplasmic, CCT chaperones were shown to also localize to the centrosome and interact with some subunits of the BBSome [42], a stable complex whose assembly and vesicle-trafficking activity regulate cilia membrane formation and composition [77, 87]. The functional association between CCT chaperones and ciliogenesis is further strengthened by findings in *Tetrahymena* showing that CCT and chaperones are required for cilia assembly as their depletion leads to axoneme shortening and splaying of MTs at its tip [41]. Nubp2 was not one of the 7 co-immunoprecipitated bands cut out from the gel and identified by MS, however when we further probed the same Nubp1 IP material by WB we could confirm the presence of Nubp2 in the protein complex (Fig. 8a3). Furthermore, although subunit CCT1 was also not one of the group of proteins identified in the Nubp1 complex, when we conducted reverse IP, using an anti-CCT1 antibody, we demonstrated that it could efficiently pull down Nubp1 (Fig. 8b). The co-precipitation of Nubp1 and Nubp2 with several members of the CCT1 complex points to a physical association and raises the possibility that the Nubps are a substrate of the complex or structural components or stably attached regulators of CCT complex activity.

Following up this association, we examined the recruitment of CCT proteins to the centrosome and basal body during Nubp1 or Nubp2 silencing and other silencing regimes. We found CCT8 and CCT4 properly recruited to both centrioles in cycling cells and to the basal body in serum deprived cells in Nubp1, Nubp2, KIFC5A, and double KIFC5A + Nubp1-silenced cells, similar to controls (Fig. S15A–E for CCT8; F-G for CCT4). This indicated that the presence/activity of Nubp1, Nubp2 and KIFC5A in centrioles and basal bodies is not important for targeting of the CCT complex to centrioles and the basal body. The same was the case with BBS7, a component of the BBSome complex which is part of the BBSome-CCT chaperone complex that is required for BBSome assembly [42, 77, 88], and which we found to correctly localize to basal bodies in the absence of Nubp1, Nubp2, or KIFC5A + Nubp1 (Fig. S15H–K).

Discussion

In this work, we provide new evidence for the functional role of Nubp1 and Nubp2 and their interacting motor

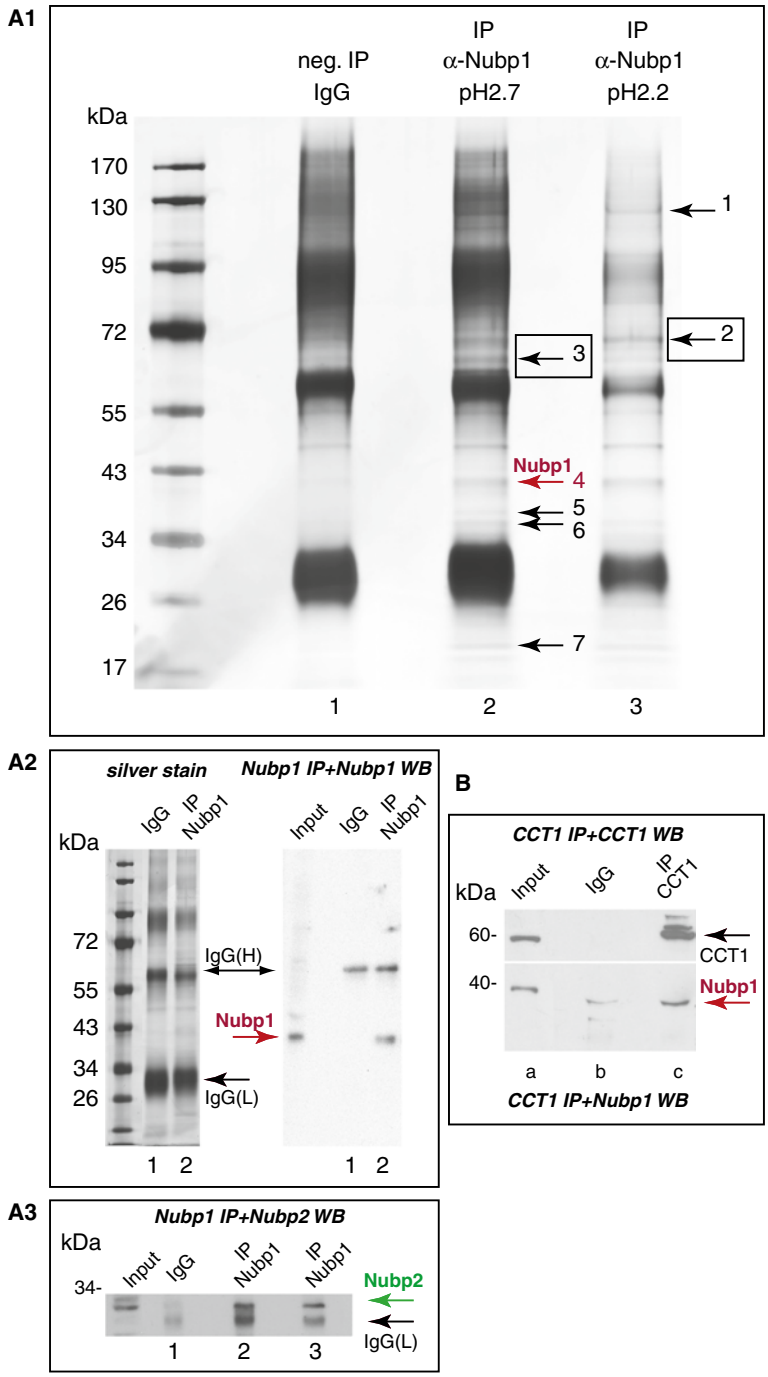

Fig. 8 Nubp1 IP and reverse IP for the identification of interacting proteins in mouse. **a1** Silver-stained SDS-PAGE gel showing control IP (*lane 1*), IP with the use of affinity-purified anti-Nubp1 ab and bound proteins eluted at pH 2.7 (*lane 2*), or eluted at pH 2.2 (*lane 3*). Bands uniquely present in Nubp1 IPs (bands 1–7, indicated by *arrows*) were isolated and identified by LC–MS/MS. The results are shown in Table S2. Band no. 4 corresponds to Nubp1, while bands 2 and 3 correspond to CCT complex chaperones CCT3-8. **a2**–**a3** Analysis of Nubp1 IP and negative control IP samples of equal protein concentration by silver staining (panel **a2**, *left*), or WB with anti-Nubp1 (panel **a2**, *right*) or anti-Nubp2 antibodies (panel **a3**). This confirms the presence of Nubp2 in the Nubp1 IP complex. *Lanes 1–3* are as in panel **a1**. Note that 40 % of the IP material was used in panel **a1**, 10 % each for panels **a2** and **a3**, and 20 % for panel **a4**. **b** Western-blot analysis of a CCT1 IP experiment, using an adult-mouse brain extract, probed with either CCT1 (*top panel*) or Nubp1 antibodies (*bottom panel*), demonstrating that the CCT1 antibody can effectively co-immunoprecipitate Nubp1. Lanes: *a* is an input sample, *b* is the rat IgG negative control IP, *c* is the CCT1 affinity-purified rat antibody IP

protein KIFC5A in the formation of primary cilia. We document the first definitive intracellular localization of endogenous Nubp1 and Nubp2 in vertebrate cells, thus avoiding the artifactual and unspecific cytoplasmic and nuclear accumulation of reporter-tagged Nubp proteins observed by us (for GFP-, myc-, or FLAG-tagged Nubp1 or Nubp2; data not shown), and others [89]. In cycling cells, the Nubp proteins are co-localized as stably integrated components of mitotic and interphase centrioles and associated with spindle MTs (Figs. 1, 2, S2–S3). In quiescent cells they are found in the basal body; immunogold EM for Nubp1 reveals labeling at the basal body and its accessory structures as well as an association with outer doublet MTs at the periphery of the ciliary axoneme of motile cilia (Figs. 2, 3, S4). Consistently, biochemical analysis reveals that Nubp1 primarily associates with the axonemal fraction of flagella, although some is present in the detergent-extractable fraction (Fig. 4). Following the functional implication of KIFC5A, Nubp1, and Nubp2 in the regulation of centriole duplication in mammalian cells by our previous work

[49], the present study shows that all three proteins have differential effects in ciliogenesis (summarized in Table S3). While the downregulation of KIFC5A by RNAi drastically reduces the percentage of ciliated cells, the depletion of either Nubp1 or Nubp2 causes significant increase of ciliogenesis (Fig. 6). In line with these results, in mouse cells Nubp1 and Nubp2 are significantly downregulated when ciliogenesis is induced by serum deprivation (Fig. S11). We demonstrate that both the localization of Nubp1 as well as its impact as a regulator of ciliogenesis, appear to be phylogenetically conserved in vertebrates and invertebrates (Fig. 5, S6). The basal bodies that form during depletion of Nubp1 or Nubp2 or KIFC5A or Nubp1 + KIFC5A in mouse cells are able to recruit normally protein components that are critically important for ciliogenesis (Chibby, Cenexin, CP110, CEP290, Rab8, AurA, and BBS7) (Figs. 7, S12-S14). What could be the molecular basis of the involvement of Nubp1 and Nubp2 in ciliogenesis?

Here we demonstrate by IP/MS that Nubp1 interacts with six of the eight constituents of the CCT/TRiC chaperone complex, chaperonins CCT3-CCT8 and, additionally, in the reverse IP, Nubp1 is effectively co-immunoprecipitated by the CCT1 antibody (Fig. 8a1, a2, b; Table S2). This indicates that Nubp1 as well as Nubp2, also detectable in the same IP reaction (Fig. 8a3), are part of the CCT/TRiC complex or stably associated with it or even its substrates. The absence of CCT1 (albeit confirmed as Nubp1-interacting by CCT1 IP) and CCT2 in our MS analysis most likely results from their differential migration on the gel in bands that were not detectable as discernible entities and/or were not analyzed. Alternatively, this may correspond to a distinct complex engaging a subgroup of CCTs together with Nubp1, as it is documented that CCTs may form different complexes, other than the main CCT particle, for example in association with certain BBS proteins [42]. We found that depletion of Nubp1, Nubp2, KIFC5A, or the combination of Nubp1 + KIFC5A does not interfere with the basal body recruitment of CCTs (Fig. S15). Group II chaperonins are conserved in all three domains of life, and it is estimated that 5–10 % of all newly synthesized proteins are assisted in their folding by the CCT complex [84, 90]. Binding and hydrolysis of ATP to the subunits of the CCT complex are essential for folding of protein substrates [91], and they have been suggested as "regulatory switches" for the binding of target proteins to the CCT [92]. Interestingly, recognition of target proteins by the CCT complex for the final steps of folding often requires the previous upstream activity of a co-chaperonin (for example prefoldin or phosducin-like proteins) to reach an intermediate, quasi-native, conformation [93]. The involvement of more than one class of molecular chaperones, working in concert and generating a "protective passageway" in the folding of multidomain proteins, seems to be a typical pattern of action [34]. CCT chaperonins are also found to be involved in the intermediate maturation steps of multiprotein assemblies, like complexes involving subsets of BBSome proteins before full BBSome assembly in cilia [42, 88] and chromatin remodeling complexes [94]. CCT chaperonins are abundant in the cytoplasm but almost all of them are specifically enriched at the centrosome [42] and, as we show here, also at the basal body.

In order to reconcile the different biological processes in which Nubp1 has been implicated, namely cytosolic Fe/S protein biogenesis [52–55] and centriole duplication [49], with ciliogenesis, CCT association and the other functional data presented in the current work, a role could be proposed for Nubp1 as a chaperone co-factor, involved in different protein–protein interactions, be it as a member of the CCT complex (or an alternative CCT-containing complex) in cilia or, conceivably, also in other chaperone complexes. Given Nubp1 interaction and co-localization with Nubp2 [49, 53], their similar effects in ciliogenesis and their co-detection in the Nubp1-immunoprecipitated and CCT-containing complex, it is likely that the two proteins function as a complex in vivo. The relatively modest abundance of Nubp1 in cells, its association with CCT chaperonins and scaffold complexes [53], and its diverse functions, may point to a catalytic function, in concert with a chaperone activity. Interestingly in this context, in a yeast two-hybrid screen for mouse Nubp1 novel protein interactions that we carried out (Santama, unpublished), we identified, among other hits, tubulin beta-5 (tubb5; NM_011655.4) as a Nubp1-interacting protein. This putative interaction would tie in with the observed association of Nubp1 with MTs, both in the mitotic spindle and the ciliary axoneme and, possibly, at the basal body as well (Figs. 1, 2, 3). Nubp1, in a proposed role of a multi-tasking molecular chaperone co-factor, could interact with different proteins or protein complexes to affect their folding or modify their activity, acting independently or in co-ordination with molecular chaperones, and thus contributing to the regulation of different biological processes. It is plausible that at the centriole, for example, Nubp1 through its enzymatic activity on β-tubulin folding or binding of MT components may regulate MT polymerization and stability of precursors destined for cilia and, as a negative regulator of ciliogenesis, thus prevent premature ciliary assembly at an inappropriate time and until the ciliogenesis program is activated. When Nubp1 is downregulated (at the onset and during ciliogenesis) or silenced by RNAi, such interactions are reduced, allowing ciliogenesis to proceed. Actin is another major substrate of the CCT complex [36] and the actin cytoskeleton is important for ciliogenesis [95, 96]. It is therefore interesting that new findings link Nubp1 with the organization and stability of the dense apical actin meshwork, anchoring the arrays of basal bodies that organize the motile cilia in multiciliated

epidermal cells in *Xenopus* [97]. Additionally, a strong link is emerging from recent studies [98] between the state of polymerization of the actin and tubulin networks and cilium length; in particular, the increase in cilia length is directly correlated with the levels of soluble tubulin. The here-proposed role for Nubp1, acting on different protein substrates as regulator, is compatible with its involvement in distinct biological processes and the observation that in its absence both the centrioles and cilia seem to form properly but in an unregulated manner (overduplication for centrioles in cycling cells, enhanced ciliogenesis in quiescent cells). In our MS analysis of Nubp1-immunoprecipitated complexes, we identified several other proteins (Table S2) and will be analyzing these putative interactions further; again these may point to the involvement of Nubp1 in novel, as yet uncharacterized, further cellular functions.

Regarding the possible involvement of KIFC5A in ciliogenesis, one could argue that the effects of its depletion in reducing the percentage of ciliated cells might be indirect or independent from its association with the Nubp proteins. However, the observation that co-silencing of KIFC5A and Nubp1 appears to negate the single effect of the depletion of each of the proteins independently on the one hand, and their established physical interaction and similar effects on centriole arithmetics on the other [49], points to a likely functional association between the two proteins in ciliogenesis also. Our current work indicates that Nubp1 and Nubp2 are most likely not substrates of KIFC5A-mediated translocation, given their KIFC5A-independent recruitment to centrioles and the basal body (Fig. S5), and their effects on ciliogenesis, which are opposite of that of KIFC5A silencing (Fig. 6). Our new data allow an interpretation of the involvement of KIFC5A, a minus end-directed molecular motor, in ciliogenesis, taking into account that the protein is undetectable on interphase centrioles, the basal body and the ciliary axoneme (Fig. 2), an indication that KIFC5A does not accumulate there in significant concentrations.

KIFC5A is highly enriched in mitotic centrioles and spindle MTs and, despite the lack of obvious defects in centriole maturation as judged by IF with several centrosome proteins, it could thus serve during mitosis in the timely transport/enrichment of proteins that are essential for the transformation of the mother centriole to basal body upon mitotic exit. For example, the function of BBS6, a core component of centrosomes, is dependent on its correct centrosomal targeting, which is significantly enriched during mitosis [39]. BBS6, itself an atypical molecular chaperone with type II chaperonin homology, mediates the association of BBS7 protein with CCT chaperones and is essential for both BBSome assembly and ciliogenesis [42]. Intriguingly, RNAi-mediated depletion of BBS6 causes centrosome amplification, cytokinesis defects and multinucleation [39], a phenotype akin to the phenotype observed upon silencing of KIFC5A [49]. Therefore, KIFC5A could be involved in the transport of proteins whose enrichment is essential for ciliogenesis, like BBS6, on mitotic centrioles.

In addition to the established role of motor proteins in IFT ("Introduction"), new information is emerging on their involvement in ciliogenesis through their MT-modifying activity. For example, KIF24, a kinesin-13 motor localizing to centrioles, influences ciliogenesis in two distinct ways: by recruiting CP110, a ciliogenesis repressor, to the distal tip of centrioles and also by regulating MT assembly and remodeling MTs, by virtue of its depolymerizing activity, specifically at the vicinity of the basal body [99]. Furthermore, *Chlamydomonas* kinesin-13 is regulated via reversible phosphorylation in the cytoplasm, and functions in both disassembly and re-assembly of flagella during regeneration, indicating that MT dynamics in the cell body may be as important for flagellar growth and length as MT dynamics in the flagellum itself [100]. KIFC5A, like other kinesin-14 motors, possesses MT crosslinking (bundling) activity [49]. It therefore has the scope to mediate its effects on ciliogenesis both by recruitment of other protein factors or by MT crosslinking and the corresponding modification of MT dynamics. Both aspects of KIFC5A functionality, however, have not been specifically addressed here.

Finally, an interesting result from our studies is that the differences that we recorded in the ciliogenesis capacity of cells silenced for different proteins (for example KIFC5A vs. Nubp1) were maintained independently of the number of centrioles they contained. KIFC5A-silenced cells consistently generated fewer cilia than controls, regardless of whether they possessed two or more centrioles. Conversely, Nubp1-silenced cells were more ciliogenic than controls, whether or not they had the normal or an amplified centriole content (Table 1). Additionally, the frequency of ciliated cells with multiple centrioles in each of the groups was essentially the same as in the corresponding non-ciliated fraction of the same group, indicating that the state of centriole amplification was not per se refractory to ciliation. In essence, our data show that multicentriolation neither decreases nor increases the number of primary cilia per cell. Taken together, these results are consistent with the notion that ciliation is centriole-driven and that the centriole has an intrinsic ciliogenesis potential, which appears independent of the total number of centrioles per cell. This conclusion is in agreement with studies using Plk4 overexpression to induce multicentrioled cells, which were able to generate cilia and, often, more than one, indicating that the state of multicentriolation could effectively support ciliogenesis [46]. Interestingly, these supernumerary cilia had reduced concentrations of signaling molecules and compromised signaling capacity most likely as a result of sharing the same ciliary pocket and, consequently, the same pool of proteins targeted to the cilium. Such multicentrioled and

multiciliated cells had a reduced ability to support epithelial organization in 3D spheroid cultures. In another study [101], a mouse strain harboring point mutations in its Nubp1 gene exhibited syndactyly, cataract and lung hypoplasia, symptoms partially overlapping with those of ciliopathies, while Nubp1 knockdown in lung epithelial cell cultures caused centriole amplification, similar to our original observations in NIH 3T3 fibroblasts [49]. While cilia were not specifically examined in mutant animals [101], the possibility that they may possess multiciliated lung epithelial cells, similar to multiciliated cells from tuberous sclerosis patients [46], may explain the lung hypoplasia and other developmental abnormalities observed.

Acknowledgments We warmly thank our colleagues for kindly providing antibodies: Profs. Ryoko Kuriyama (University of Minnesota), Anand Swaroop (NIH, Bethesda), Isabelle Vernos (CRG, Barcelona), Johan Peränen (University of Helsinki), Joel Rosenbaum (Yale University) and Elizabeth Smith (Dartmouth College, NH). We are indebted to Ioanna Georgiou and Maria Christoforou (University of Cyprus) for cell-cycle analysis of Nubp1 and to Elena Panayiotou-Worth (Cyprus Institute of Neurology and Genetics) for providing us with mouse tracheal sections. This work was funded by the Research Promotion Foundation of Cyprus and Structural Funds from the EU (grant DIDAKTOR/DISEK/0308-05 to N.S.) and the Danish Natural Science Research Council (grants 09-070398 and 10-085373 to L.B.P.). E.K. received a FEBS short-term fellowship to visit the laboratory of N.T. for work with *C. elegans*.

References

1. Dawe HR, Farr H, Gull K (2007) Centriole/basal body morphogenesis and migration during ciliogenesis in animal cells. J Cell Sci 120(Pt 1):7–15
2. Pedersen LB, Veland IR, Schroder JM, Christensen ST (2008) Assembly of primary cilia. Dev Dyn 237(8):1993–2006
3. Gerdes JM, Davis EE, Katsanis N (2009) The vertebrate primary cilium in development, homeostasis, and disease. Cell 137(1):32–45
4. Satir P, Pedersen LB, Christensen ST (2010) The primary cilium at a glance. J Cell Sci 123(Pt 4):499–503
5. Seeley ES, Nachury MV (2010) The perennial organelle: assembly and disassembly of the primary cilium. J Cell Sci 123(Pt 4):511–518
6. Christensen ST, Pedersen LB, Schneider L, Satir P (2007) Sensory cilia and integration of signal transduction in human health and disease. Traffic 8(2):97–109
7. Wong SY, Seol AD, So PL, Ermilov AN, Bichakjian CK, Epstein EH Jr, Dlugosz AA, Reiter JF (2009) Primary cilia can both mediate and suppress Hedgehog pathway-dependent tumorigenesis. Nat Med 15(9):1055–1061
8. Goetz SC, Anderson KV (2010) The primary cilium: a signalling centre during vertebrate development. Nat Rev Genet 11(5):331–344
9. Wallingford JB, Mitchell B (2011) Strange as it may seem: the many links between Wnt signaling, planar cell polarity, and cilia. Genes Dev 25(3):201–213
10. Hoyer-Fender S (2010) Centriole maturation and transformation to basal body. Semin Cell Dev Biol 21(2):142–147
11. Yang J, Gao J, Adamian M, Wen XH, Pawlyk B, Zhang L, Sanderson MJ, Zuo J, Makino CL, Li T (2005) The ciliary rootlet maintains long-term stability of sensory cilia. Mol Cell Biol 25(10):4129–4137
12. Anderson RG (1972) The three-dimensional structure of the basal body from the rhesus monkey oviduct. J Cell Biol 54(2):246–265
13. Deane JA, Cole DG, Seeley ES, Diener DR, Rosenbaum JL (2001) Localization of intraflagellar transport protein IFT52 identifies basal body transitional fibers as the docking site for IFT particles. Curr Biol 11(20):1586–1590
14. Hu Q, Milenkovic L, Jin H, Scott MP, Nachury MV, Spiliotis ET, Nelson WJ (2010) A septin diffusion barrier at the base of the primary cilium maintains ciliary membrane protein distribution. Science 329(5990):436–439
15. Dishinger JF, Kee HL, Jenkins PM, Fan S, Hurd TW, Hammond JW, Truong YN, Margolis B, Martens JR, Verhey KJ (2010) Ciliary entry of the kinesin-2 motor KIF17 is regulated by importin-beta2 and RanGTP. Nat Cell Biol 12(7):703–710
16. Spektor A, Tsang WY, Khoo D, Dynlacht BD (2007) Cep97 and CP110 suppress a cilia assembly program. Cell 130(4):678–690
17. Tsang WY, Bossard C, Khanna H, Peranen J, Swaroop A, Malhotra V, Dynlacht BD (2008) CP110 suppresses primary cilia formation through its interaction with CEP290, a protein deficient in human ciliary disease. Dev Cell 15(2):187–197
18. Kim J, Krishnaswami SR, Gleeson JG (2008) CEP290 interacts with the centriolar satellite component PCM-1 and is required for Rab8 localization to the primary cilium. Hum Mol Genet 17(23):3796–3805
19. Pugacheva EN, Jablonski SA, Hartman TR, Henske EP, Golemis EA (2007) HEF1-dependent Aurora A activation induces disassembly of the primary cilium. Cell 129(7):1351–1363
20. Wei Q, Zhang Y, Li Y, Zhang Q, Ling K, Hu J (2012) The BBSome controls IFT assembly and turnaround in cilia. Nat Cell Biol 14(9):950–957
21. Ou G, Blacque OE, Snow JJ, Leroux MR, Scholey JM (2005) Functional coordination of intraflagellar transport motors. Nature 436(7050):583–587
22. Scholey JM, Anderson KV (2006) Intraflagellar transport and cilium-based signaling. Cell 125(3):439–442
23. Pedersen LB, Rosenbaum JL (2008) Intraflagellar transport (IFT) role in ciliary assembly, resorption and signalling. Curr Top Dev Biol 85:23–61
24. Silverman MA, Leroux MR (2009) Intraflagellar transport and the generation of dynamic, structurally and functionally diverse cilia. Trends Cell Biol 19(7):306–316
25. Karsenti E, Vernos I (2001) The mitotic spindle: a self-made machine. Science 294(5542):543–547
26. Johnson KA, Rosenbaum JL (1992) Polarity of flagellar assembly in *Chlamydomonas*. J Cell Biol 119(6):1605–1611
27. Marshall WF, Rosenbaum JL (2001) Intraflagellar transport balances continuous turnover of outer doublet microtubules: implications for flagellar length control. J Cell Biol 155(3):405–414
28. Akhmanova A, Steinmetz MO (2008) Tracking the ends: a dynamic protein network controls the fate of microtubule tips. Nat Rev Mol Cell Biol 9(4):309–322
29. Schuyler SC, Pellman D (2001) Microtubule "plus-end-tracking proteins": the end is just the beginning. Cell 105(4):421–424
30. Vaughan KT (2005) TIP maker and TIP marker; EB1 as a master controller of microtubule plus ends. J Cell Biol 171(2):197–200
31. Schrøder JM, Schneider L, Christensen ST, Pedersen LB (2007) EB1 is required for primary cilia assembly in fibroblasts. Curr Biol 17(13):1134–1139
32. Schrøder JM, Larsen J, Komarova Y, Akhmanova A, Thorsteinsson RI, Grigoriev I, Manguso R, Christensen ST, Pedersen SF, Geimer S, Pedersen LB (2011) EB1 and EB3 promote cilia

biogenesis by several centrosome-related mechanisms. J Cell Sci 124(Pt 15):2539–2551
33. Horwich AL, Fenton WA, Chapman E, Farr GW (2007) Two families of chaperonin: physiology and mechanism. Annu Rev Cell Dev Biol 23:115–145
34. Kabir MA, Uddin W, Narayanan A, Reddy PK, Jairajpuri MA, Sherman F, Ahmad Z (2011) Functional subunits of eukaryotic chaperonin CCT/TRiC in protein folding. J Amino Acids 2011:843206
35. Yaffe MB, Farr GW, Miklos D, Horwich AL, Sternlicht ML, Sternlicht H (1992) TCP1 complex is a molecular chaperone in tubulin biogenesis. Nature 358(6383):245–248
36. Gao Y, Thomas JO, Chow RL, Lee GH, Cowan NJ (1992) A cytoplasmic chaperonin that catalyzes beta-actin folding. Cell 69(6):1043–1050
37. Melki R, Vainberg IE, Chow RL, Cowan NJ (1993) Chaperonin-mediated folding of vertebrate actin-related protein and gamma-tubulin. J Cell Biol 122(6):1301–1310
38. Bloch MA, Johnson KA (1995) Identification of a molecular chaperone in the eukaryotic flagellum and its localization to the site of microtubule assembly. J Cell Sci 108(Pt 11):3541–3545
39. Kim JC, Ou YY, Badano JL, Esmail MA, Leitch CC, Fiedrich E, Beales PL, Archibald JM, Katsanis N, Rattner JB, Leroux MR (2005) MKKS/BBS6, a divergent chaperonin-like protein linked to the obesity disorder Bardet–Biedl syndrome, is a novel centrosomal component required for cytokinesis. J Cell Sci 118(Pt 5):1007–1020
40. Blacque OE, Perens EA, Boroevich KA, Inglis PN, Li C, Warner A, Khattra J, Holt RA, Ou G, Mah AK, McKay SJ, Huang P, Swoboda P, Jones SJ, Marra MA, Baillie DL, Moerman DG, Shaham S, Leroux MR (2005) Functional genomics of the cilium, a sensory organelle. Curr Biol 15(10):935–941
41. Seixas C, Cruto T, Tavares A, Gaertig J, Soares H (2010) CCTalpha and CCTdelta chaperonin subunits are essential and required for cilia assembly and maintenance in *Tetrahymena*. PLoS One 5(5):e10704
42. Seo S, Baye LM, Schulz NP, Beck JS, Zhang Q, Slusarski DC, Sheffield VC (2010) BBS6, BBS10, and BBS12 form a complex with CCT/TRiC family chaperonins and mediate BBSome assembly. Proc Natl Acad Sci USA 107(4):1488–1493
43. Plotnikova OV, Golemis EA, Pugacheva EN (2008) Cell cycle-dependent ciliogenesis and cancer. Cancer Res 68(7):2058–2061
44. Godinho SA, Kwon M, Pellman D (2009) Centrosomes and cancer: how cancer cells divide with too many centrosomes. Cancer Metastasis Rev 28(1–2):85–98. doi:10.1007/s10555-008-9163-6
45. Hatch E, Stearns T (2010) The life cycle of centrioles. Cold Spring Harb Symp Quant Biol 75:425–431
46. Mahjoub MR, Stearns T (2012) Supernumerary centrosomes nucleate extra cilia and compromise primary cilium signaling. Curr Biol 22(17):1628–1634
47. Shahrestanifar M, Saha DP, Scala LA, Basu A, Howells RD (1994) Cloning of a human cDNA encoding a putative nucleotide-binding protein related to *Escherichia coli* MinD. Gene 147(2):281–285
48. Nakashima H, Grahovac MJ, Mazzarella R, Fujiwara H, Kitchen JR, Threat TA, Ko MS (1999) Two novel mouse genes–Nubp2, mapped to the t-complex on chromosome 17, and Nubp1, mapped to chromosome 16–establish a new gene family of nucleotide-binding proteins in eukaryotes. Genomics 60(2):152–160
49. Christodoulou A, Lederer CW, Surrey T, Vernos I, Santama N (2006) Motor protein KIFC5A interacts with Nubp1 and Nubp2, and is implicated in the regulation of centrosome duplication. J Cell Sci 119(Pt 10):2035–2047
50. Leipe DD, Wolf YI, Koonin EV, Aravind L (2002) Classification and evolution of P-loop GTPases and related ATPases. J Mol Biol 317(1):41–72
51. Vitale G, Fabre E, Hurt EC (1996) NBP35 encodes an essential and evolutionary conserved protein in *Saccharomyces cerevisiae* with homology to a superfamily of bacterial ATPases. Gene 178(1–2):97–106
52. Hausmann A, Aguilar Netz DJ, Balk J, Pierik AJ, Muhlenhoff U, Lill R (2005) The eukaryotic P loop NTPase Nbp35: an essential component of the cytosolic and nuclear iron-sulfur protein assembly machinery. Proc Natl Acad Sci USA 102(9):3266–3271
53. Netz DJ, Pierik AJ, Stumpfig M, Muhlenhoff U, Lill R (2007) The Cfd1-Nbp35 complex acts as a scaffold for iron-sulfur protein assembly in the yeast cytosol. Nat Chem Biol 3(5):278–286
54. Stehling O, Netz DJ, Niggemeyer B, Rosser R, Eisenstein RS, Puccio H, Pierik AJ, Lill R (2008) Human Nbp35 is essential for both cytosolic iron-sulfur protein assembly and iron homeostasis. Mol Cell Biol 28(17):5517–5528
55. Netz DJ, Pierik AJ, Stumpfig M, Bill E, Sharma AK, Pallesen LJ, Walden WE, Lill R (2012) A bridging [4Fe-4S] cluster and nucleotide binding are essential for function of the Cfd1-Nbp35 complex as a scaffold in iron-sulfur protein maturation. J Biol Chem 287(15):12365–12378
56. Pedersen LB, Geimer S, Sloboda RD, Rosenbaum JL (2003) The microtubule plus end-tracking protein EB1 is localized to the flagellar tip and basal bodies in *Chlamydomonas reinhardtii*. Curr Biol 13(22):1969–1974
57. Pedersen LB, Rompolas P, Christensen ST, Rosenbaum JL, King SM (2007) The lissencephaly protein Lis1 is present in motile mammalian cilia and requires outer arm dynein for targeting to *Chlamydomonas flagella*. J Cell Sci 120(Pt 5):858–867
58. D'Angiolella V, Donato V, Vijayakumar S, Saraf A, Florens L, Washburn MP, Dynlacht B, Pagano M (2010) SCF(Cyclin F) controls centrosome homeostasis and mitotic fidelity through CP110 degradation. Nature 466(7302):138–142
59. Rieckher M, Kourtis N, Pasparaki A, Tavernarakis N (2009) Transgenesis in *Caenorhabditis elegans*. Methods Mol Biol 561:21–39
60. Troemel ER, Kimmel BE, Bargmann CI (1997) Reprogramming chemotaxis responses: sensory neurons define olfactory preferences in *C. elegans*. Cell 91(2):161–169
61. Kamath RS, Martinez-Campos M, Zipperlen P, Fraser AG, Ahringer J (2001) Effectiveness of specific RNA-mediated interference through ingested double-stranded RNA in *Caenorhabditis elegans*. Genome Biol 2 (1):RESEARCH0002
62. Gorman DS, Levine RP (1965) Cytochrome f and plastocyanin: their sequence in the photosynthetic electron transport chain of *Chlamydomonas reinhardi*. Proc Natl Acad Sci USA 54(6):1665–1669
63. Cole DG, Diener DR, Himelblau AL, Beech PL, Fuster JC, Rosenbaum JL (1998) Chlamydomonas kinesin-II-dependent intraflagellar transport (IFT): IFT particles contain proteins required for ciliary assembly in *Caenorhabditis elegans* sensory neurons. J Cell Biol 141(4):993–1008
64. Ahmed NT, Gao C, Lucker BF, Cole DG, Mitchell DR (2008) ODA16 aids axonemal outer row dynein assembly through an interaction with the intraflagellar transport machinery. J Cell Biol 183(2):313–322
65. Pedersen LB, Geimer S, Rosenbaum JL (2006) Dissecting the molecular mechanisms of intraflagellar transport in *Chlamydomonas*. Curr Biol 16(5):450–459. doi:10.1016/j.cub.2006.02.020
66. Jakobsen L, Vanselow K, Skogs M, Toyoda Y, Lundberg E, Poser I, Falkenby LG, Bennetzen M, Westendorf J, Nigg

EA, Uhlen M, Hyman AA, Andersen JS (2011) Novel asymmetrically localizing components of human centrosomes identified by complementary proteomics methods. EMBO J 30(8):1520–1535
67. Pazour GJ, Agrin N, Leszyk J, Witman GB (2005) Proteomic analysis of a eukaryotic cilium. J Cell Biol 170:103–113
68. Dymek EE, Goduti D, Kramer T, Smith EF (2006) A kinesin-like calmodulin-binding protein in *Chlamydomonas*: evidence for a role in cell division and flagellar functions. J Cell Sci 119(Pt 15):3107–3116
69. Bargmann CI, Mori I (1997) Chemotaxis and thermotaxis. In: Riddle DL, Blumenthal T, Meyer BJ, Priess JR (eds) C. elegans II, 2nd edn. Cold Spring Harbor Laboratory Press, Cold Spring Harbor, NY
70. Driscoll M, Kaplan J (1997) Mechanotransduction. In: Riddle DL, Blumenthal T, Meyer BJ, Priess JR (eds) C. elegans II, 2nd edn. Cold Spring Harbor Laboratory Press, Cold Spring Harbor, NY
71. Riddle DL, Albert PS (1997) Genetic and environmental regulation of dauer larva development. In: Riddle DL, Blumenthal T, Meyer BJ, Priess JR (eds) C. elegans II, 2nd edn. Cold Spring Harbor Laboratory Press, Cold Spring Harbor, NY
72. Hilliard MA, Bargmann CI, Bazzicalupo P (2002) *C. elegans* responds to chemical repellents by integrating sensory inputs from the head and the tail. Curr Biol 12(9):730–734
73. Takemaru K, Yamaguchi S, Lee YS, Zhang Y, Carthew RW, Moon RT (2003) Chibby, a nuclear beta-catenin-associated antagonist of the Wnt/Wingless pathway. Nature 422(6934):905–909
74. Steere N, Chae V, Burke M, Li FQ, Takemaru K, Kuriyama R (2012) A Wnt/beta-catenin pathway antagonist Chibby binds cenexin at the distal end of mother centrioles and functions in primary cilia formation. PLoS One 7(7):e41077
75. Chen Z, Indjeian VB, McManus M, Wang L, Dynlacht BD (2002) CP110, a cell cycle-dependent CDK substrate, regulates centrosome duplication in human cells. Dev Cell 3(3):339–350
76. Kleylein-Sohn J, Westendorf J, Le Clech M, Habedanck R, Stierhof YD, Nigg EA (2007) Plk4-induced centriole biogenesis in human cells. Dev Cell 13:190–202
77. Nachury MV, Loktev AV, Zhang Q, Westlake CJ, Peranen J, Merdes A, Slusarski DC, Scheller RH, Bazan JF, Sheffield VC, Jackson PK (2007) A core complex of BBS proteins cooperates with the GTPase Rab8 to promote ciliary membrane biogenesis. Cell 129(6):1201–1213
78. Yoshimura S, Egerer J, Fuchs E, Haas AK, Barr FA (2007) Functional dissection of Rab GTPases involved in primary cilium formation. J Cell Biol 178(3):363–369
79. Peränen J (2011) Rab8 GTPase as a regulator of cell shape. Cytoskeleton (Hoboken) 68(10):527–539
80. Salisbury JL, Suino KM, Busby R, Springett M (2002) Centrin-2 is required for centriole duplication in mammalian cells. Curr Biol 12(15):1287–1292
81. Kubota H, Hynes G, Willison K (1995) The chaperonin containing t-complex polypeptide 1 (TCP-1). Multisubunit machinery assisting in protein folding and assembly in the eukaryotic cytosol. Eur J Biochem 230(1):3–16
82. Sternlicht H, Farr GW, Sternlicht ML, Driscoll JK, Willison K, Yaffe MB (1993) The t-complex polypeptide 1 complex is a chaperonin for tubulin and actin in vivo. Proc Natl Acad Sci USA 90(20):9422–9426
83. Dunn AY, Melville MW, Frydman J (2001) Review: cellular substrates of the eukaryotic chaperonin TRiC/CCT. J Struct Biol 135(2):176–184
84. Spiess C, Meyer AS, Reissmann S, Frydman J (2004) Mechanism of the eukaryotic chaperonin: protein folding in the chamber of secrets. Trends Cell Biol 14(11):598–604
85. Dekker C, Stirling PC, McCormack EA, Filmore H, Paul A, Brost RL, Costanzo M, Boone C, Leroux MR, Willison KR (2008) The interaction network of the chaperonin CCT. EMBO J 27(13):1827–1839
86. Camasses A, Bogdanova A, Shevchenko A, Zachariae W (2003) The CCT chaperonin promotes activation of the anaphase-promoting complex through the generation of functional Cdc20. Mol Cell 12(1):87–100
87. Lechtreck KF, Johnson EC, Sakai T, Cochran D, Ballif BA, Rush J, Pazour GJ, Ikebe M, Witman GB (2009) The *Chlamydomonas reinhardtii* BBSome is an IFT cargo required for export of specific signaling proteins from flagella. J Cell Biol 187(7):1117–1132
88. Zhang Q, Yu D, Seo S, Stone EM, Sheffield VC (2012) Intrinsic protein–protein interaction-mediated and chaperonin-assisted sequential assembly of stable Bardet–Biedl syndrome protein complex, the BBSome. J Biol Chem 287(24):20625–20635
89. Okuno T, Yamabayashi H, Kogure K (2010) Comparison of intracellular localization of Nubp1 and Nubp2 using GFP fusion proteins. Mol Biol Rep 37(3):1165–1168
90. Thulasiraman V, Yang CF, Frydman J (1999) In vivo newly translated polypeptides are sequestered in a protected folding environment. EMBO J 18(1):85–95
91. Melki R, Cowan NJ (1994) Facilitated folding of actins and tubulins occurs via a nucleotide-dependent interaction between cytoplasmic chaperonin and distinctive folding intermediates. Mol Cell Biol 14(5):2895–2904
92. Melki R (2001) Review: nucleotide-dependent conformational changes of the chaperonin containing TCP-1. J Struct Biol 135(2):170–175
93. Tian G, Vainberg IE, Tap WD, Lewis SA, Cowan NJ (1995) Quasi-native chaperonin-bound intermediates in facilitated protein folding. J Biol Chem 270(41):23910–23913
94. Guenther MG, Yu J, Kao GD, Yen TJ, Lazar MA (2002) Assembly of the SMRT-histone deacetylase 3 repression complex requires the TCP-1 ring complex. Genes Dev 16(24):3130–3135
95. Dawe HR, Adams M, Wheway G, Szymanska K, Logan CV, Noegel AA, Gull K, Johnson CA (2009) Nesprin-2 interacts with meckelin and mediates ciliogenesis via remodelling of the actin cytoskeleton. J Cell Sci 122(Pt 15):2716–2726
96. Kim J, Lee JE, Heynen-Genel S, Suyama E, Ono K, Lee K, Ideker T, Aza-Blanc P, Gleeson JG (2010) Functional genomic screen for modulators of ciliogenesis and cilium length. Nature 464(7291):1048–1051
97. Ioannou A, Santama N, Skourides P (2013) *Xenopus laevis* nucleotide-binding protein 1 (xNubp1) is important for convergent extension movements and controls ciliogenesis via regulation of the actin cytoskeleton. Dev Biol. doi:10.1016/j.ydbio.2013.05.004. [Epub ahead of print]
98. Sharma N, Kosan ZA, Stallworth JE, Berbari NF, Yoder BK (2011) Soluble levels of cytosolic tubulin regulate ciliary length control. Mol Biol Cell 22(6):806–816
99. Kobayashi T, Dynlacht BD (2011) Regulating the transition from centriole to basal body. J Cell Biol 193(3):435–444
100. Piao T, Luo M, Wang L, Guo Y, Li D, Li P, Snell WJ, Pan J (2009) A microtubule depolymerizing kinesin functions during both flagellar disassembly and flagellar assembly in *Chlamydomonas*. Proc Natl Acad Sci USA 106(12):4713–4718
101. Schnatwin C, Niswander L (2012) Nubp1 is required for lung branching morphogenesis and distal progenitor cell survival in mice. PLoS One 7(9):e44871
102. Perdiz D, Mackeh R, Poüs C, Baillet A (2011) The ins and outs of tubulin acetylation: more than just a post-translational modification? Cell Signal 23(5):763–771
103. Piperno G, LeDizet M, Chang XJ (1987) Microtubules containing acetylated alpha-tubulin in mammalian cells in culture. J Cell Biol 104(2):289–302